Investigating Parkinson Disease-Linked Alpha-Synuclein as an Anti-Viral Protein

Allison MacDonald

A thesis submitted to the Faculty of Medicine for the partial fulfillment of the requirements for the Master's of Science degree in Cellular and Molecular Medicine

July 11th, 2024

Department of Cellular and Molecular Medicine

Faculty of Medicine

University of Ottawa

Abstract

The accumulation of insoluble, α-synuclein (aSyn)-rich Lewy bodies within surviving nerve cells is considered a hallmark of Parkinson disease (PD). It is thought that changes in the protein's metabolism, including its aggregation and sustained phosphorylation at serine 129, are linked to PD pathogenesis. Previously, Braak *et al*. theorized that microbial infections could constitute environmental factors contributing to PD development. Previously, we and others have shown that wild-type aSyn confers partial protection of mice against invasion by select bacteria and RNA viruses. Here, I hypothesized that aSyn metabolism is altered in response to microbial infections and that PD-linked mutations in aSyn modify this response. Vesicular Stomatitis Virus (VSV) causes systemic infections, leading to encephalitis in rodents. In the present study, infections of neural cell lines by a GFP-expressing VSV variant were used to: 1) explore possible anti-viral properties of aSyn and identify potential differences between select aSyn mutants; and 2) monitor changes in the protein's metabolism following viral infection. When comparing the possible anti-viral effects of either wild-type aSyn or mutant proteins to a control arm, I observed trends but no significant difference using two neural cell culture models. When investigating the effects of wild-type VSV infection on the protein itself, I observed increased oligomerization of aSyn. Although these results did not substantiate an essential role for aSyn within neural cells' innate defence to VSV, they revealed that aSyn metabolism is altered following infection by VSV. These findings could inform concepts that explore the start of PD at epithelial host surfaces.

Table of Contents

Abstract ii

List of Tables v

List of Figures vi

List of Abbreviations vii

Acknowledgements viii

Chapter 1. Introduction 1

Parkinson Disease 1

Clinical significance and severity 1

Diagnosis and symptoms of Parkinson disease 2

Current treatments 3

Etiology of Parkinson disease 3

Disease pathology and pathogenesis 6

The prion hypothesis 7

Alpha-Synuclein 9

Protein structure and properties 10

Mutations in alpha-synuclein 11

Physiological functions of alpha-synuclein 13

PD and the Innate Immune System 14

Alpha-synuclein as an immune protein 18

VSV model for Parkinson disease: rationale and pathogenesis 21

Chapter 2. Materials and Methods 24

Cell cultures 24

PC12 Tet-off aSyn system 24

Plasmid preparation and sequencing 24

In vitro transfections 27

Fluorescent signal quantification 28

Flow cytometry 28

Western blotting 29

Live-cell imaging 30

Statistical analysis 30

Chapter 3. Results 31

Optimization and troubleshooting of a H4 neuroglioma transfection model for the study of aSyn within cellular innate immunity 31

Testing possible anti-viral properties of mutant aSyn constructs via fluorescent microscopy. 41

Flow cytometry methodology to revisit a biological effect by aSyn on VSV replication 43

Investigating the consequences of different aSyn mutations following VSV-GFP infection 54

Alterations in viral infection are not observed following VSV-GFP infection of non-human catecholamine producing cells in an aSyn Tet-off model 58

VSV-GFP infection does not elicit changes in aSyn protein expression of non-human catecholamine producing cells in an aSyn Tet-off model 61

Aggregation of aSyn is increased following viral infection with VSV in human neuronal cells 64

Chapter 4. Discussion 68

Chapter 5. Conclusion 80

Appendix 1 82

References 83

List of Tables

Table 1. Summary of constructs used to transiently transfect H4

Table 2. Summary of the comparisons between WT aSyn and respective aSyn mutations

Appendix Table 1. Troubleshooting steps taken

List of Figures

Figure 1. Optimization of VSV-GFP MOI to be used in H4 cell experiments

Figure 2. Alpha-synuclein protein structure

Figure 3. Initial screening of all aSyn constructs employed in the present study following VSV-GFP infection.

Figure 4. Fluorescent microscopy identifies large variability in GFP-signal production following VSV—GFP infection in H4 cells transiently transfected with the pcDNA3.1 vector control

Figure 5. Treatment with LPS does not interfere with VSV-GFP infection efficiency

Figure 6. The presence/absence of a triple flag in the aSyn protein sequence generated comparable results in different experimental readouts

Figure 7. pcDNA3.1 aSyn constructs do not confer protective qualities against VSV-GFP infection in H4 cells compared to the vector control via fluorescent microscopy

Figure 8. Fluorescent microscopy does not reveal protective qualities of aSyn in all tested aSyn constructs with a pDEST vector backbone compared to the vector control

Figure 9. Indirect immunofluorescence staining demonstrates trends in decreased VSV-GFP infectivity in mutated aSyn expressing H4 cells

Figure 10. Flow cytometry does not reveal protective qualities of aSyn in all tested aSyn constructs containing a pcDNA3.1 vector backbone compared to the vector control

Figure 11. No alterations in GFP-signal following VSV-GFP infection in H4 cells expressing various conformations of aSyn with a pDEST backbone are observe compared to the vector control

Figure 12. Protein expression of VSV and aSyn are not significantly altered post VSV-GFP infection in H4 cells expressing pcDNA3.1 aSyn constructs compared to the vector control

Figure 13. VSV and aSyn protein expression is not significantly altered post VSV-GFP infection in H4 cells expressing pDEST aSyn constructs compared to the vector control

Figure 14. Fluorescent microscopy analyses indicate the overexpression of aSyn does not alter VSV-GFP infections

Figure 15. The overexpression of aSyn does not produce alterations in GFP-signal following VSV-GFP infection in PC12-C4 cells via flow cytometry. The overexpression of aSyn does not alter VSV-GFP infections via flow cytometry

Figure 16. Western blot analyses do not reveal differences in VSV or aSyn protein expression following VSV-GFP infection in PC12-C4 cells

Figure 17. VSV infection promotes aSyn oligomerization.

Figure 18. Time-Lapse analysis of aSyn aggregation accumulation in H4 neuronal cells.

List of Abbreviations

aSyn: alpha-synuclein

dox: doxycycline

GFP: green fluorescent protein

gSyn: gamma-synuclein

LPS: lipopolysaccharide

LRRK2: human leucine rich repeat kinase 2

MOI: multiplicity of infection

NAC: non-amyloid component

PD: Parkinson disease

PRKN: parkin

PTM: post translational modification

SNARE: soluble NSF attachment protein receptor

SNCA: human alpha-synuclein

Snca: murine alpha-synuclein

TD3: type 3 Dearing

VEEV: Venezuelan equine encephalitis virus

VSV: vesicular stomatitis virus

WNV: West Nile virus

WT: wild-type

Acknowledgements

I would like to extend my gratitude to my supervisor, Dr. Michael Schlossmacher, for providing me with the opportunity to complete my Masters studies and partake in such exciting research. Your insights and knowledge have both encouraged me and motivated me to grow as a researcher. In the same light, I thank Dr. Julianna Tomlinson for providing such strong mentorship both before and throughout my studies. Your continued advice and eagerness to help greatly impacted the path of my studies and my future. I have learned so much and will forever be grateful for the experience to work with both of you.

To my thesis advisory committee members, Dr. Steffany Bennett and Dr. Max Rousseaux, I thank you for your expertise and counsel throughout my studies. Your ideas and knowledge contributed vastly to this project and have overall helped me to grow as a student.

I would also like to acknowledge Dr. Josée Coulombe, a research associate and invaluable mentor in the Schlossmacher lab. Your knowledge, lively personality and 'wellness cupboard' provided me with the perfect workspace to boost my creativity and thinking. I am proud to have flown under your wing. Also, to Dr. Qiubo Jang, I thank you for always providing a helping hand and maintaining organization within the lab so that I, and others, could perform experiments with the upmost efficiency. Your knowledge and background are admired and respected greatly. Equally, I thank Dr. Earl Brown, our lab's 'virology confidant'. Your knowledge and insight provided immense help in designing my experimental models and in troubleshooting roadblocks and hardships. Together, the three of you have positively contributed to the completion of my thesis project, and I will be forever grateful to have worked with you. To the rest of the MGS lab, I want to thank you for making my time in the lab more enjoyable and meaningful through your mentorship, friendship, and Second Cup trips. While the research itself is what got me through

the doors, you all are undoubtedly what helped get me out. While you will all be missed, I am so happy to have met you and will cherish the memories we have made.

It is important to me that I also extend my gratitude to Dr. Antonio Colavita. While working in your lab as an undergraduate student you encouraged me and guided me to pursue neuroscience research. The day you said, “you should really think about pursuing graduate studies, you’re good at this”, forever changed my goals and my confidence as a student. It was your encouragement that pushed me to continue my undergraduate studies overseas and return to the Ottawa Hospital Research Institute for graduate studies. You gave me a strong appreciation for the scientific field, and for tiny worms. Thank you so much.

I must also thank my family and loved ones for their continued support. I know I am always going back to school, and it would seem that being a student may just be my career. Yet, my parents never discourage me from pursuing my dreams. That means so much. To my brother Colton, I thank you for being by my side through everything and providing me with the necessary mental breaks I needed during my weekends back home. Our Marvel movie nights mean so much more than I can say. To my partner Taylor, I thank you for your support and genuine interest in my studies. You constantly challenge me to think in new ways, even when you’re an ocean away. Your support and confidence in me have made such a positive difference in my life.

Finally, to myself. I am so proud of what I have accomplished and the person I have become. I know I will continue to grow and learn; I never want to stop. If there’s one thing I want my future self to know, it will be “know that I believe in whatever you do, and I’ll do anything to see you through.”

Chapter 1. Introduction

Parkinson Disease

What is known today as Parkinson disease (PD) was first clearly described in 1817 by Dr. James Parkinson in his essay on the "shaking palsy". In his publication, he captured the clinical manifestation of involuntary tremors; however, affected individuals retained the notion of intact senses and intellect (Parkinson, 1817). This description was created based on six documented cases studied within the essay; three of which were closely examined by Dr. Parkinson himself, and three based on observations of London pedestrians (Jankovic, 2008; Kouli, Torsney and Kuan, 2018; Simon, Tanner and Brundin, 2020). It was not until fifty years later that the disease was officially named Parkinson disease by the Parisian neurologist Dr. Jean-Martin Charcot, who credited Dr. Parkinson's work but rejected the "shaking palsy" title upon his notion that not every patient possessed a tremor (Goetz, 2011). Dr. Charcot further provided a refined description of the disease through characterization of the clinical spectrum where he proposed two phenotypes ('tremorous' or 'ridgid') and differentiated PD from other neurological movement disorders (Goetz, 2011). While many insights have since been made in PD research, such as specific sites of neuronal death, decreased dopamine concentrations in the basal ganglia and the involvement of genetic mutations, there is still much to be learned in the way of disease initiation and progression. To this day, the condition remains unstoppable and incurable.

Clinical significance and severity

Currently, PD is the second most diagnosed neurodegenerative disease, affecting almost ten million people worldwide. Recent studies suggest an incidence rate of 90,000 per annum in the United States alone, which is 50% higher than previous estimates (Willis *et al*, 2022). Globally, the prevalence of PD has doubled over the past 25 years (World Health Organization, 2022). With

diagnoses occurring predominantly in males, the average age of onset is 60-70 years; however, rare cases can exhibit an earlier onset and a lesser male sex-bias (Simon *et al*, 2022; Hirsch *et al*, 2016). Few of these rare cases are diagnosed prior to age 40 years, estimated to occur at 5-10% of total cases. These monogenetic variants typically correlate with specific variations (Tysnes and Storstein, 2017). The ≥90% patient population is considered to develop the disease sporadically. The prevalence of this disease increases with age. Thus, total case numbers in the Western hemisphere are expected to increase with the aging population by greater than 50% come 2030 (Marras *et al*, 2018).

Diagnosis and symptoms of Parkinson disease

Parkinson disease is predominantly diagnosed in accordance with the clinical manifestation of motor symptoms such as bradykinesia, tremor, rigidity, and later, postural instability, although they are not specific. Such signs can be observed in other neurodegenerative diseases, bringing forth challenges for clinicians to make a correct diagnosis early in the course (Tolosa *et al,* 2021). Additionally, patients can exhibit non-motor symptoms decades prior to the manifestation of motor symptoms which are often misdiagnosed or ignored. This period of time is referred to as the prodromal period (Tolosa *et al*, 2021). During this time, symptoms including loss of smell, cognitive impairment, sleep disorders, fatigue, and constipation may arise. Notably, these patients may already undergo neurodegenerative changes, specifically in regions of the olfactory bulb, lower brainstem, and peripheral autonomic nervous system (Tolosa *et al,* 2021). Advances in biomarker research for early signs of PD has been of high interest in an attempt to provide patients with more definitive diagnoses as early as possible; however, research avenues have been unsuccessful in identifying disease at the earliest stages (Tolosa *et al,* 2021). Hence, the identification of patients at the prodromal stage remains an unmet need.

Current treatments

Due to the decrease in motor function as a result of the loss of dopaminergic neurons, many PD therapeutic approaches aim to restore dopaminergic neurotransmission in the striatum (Stoker and Barker, 2020). These approaches are often effective in improving motor function; however, they may come with significant side effects later on. It is noted that patients often develop cognitive issues, on/off fluctuations, and levodopa-induced dyskinesias (Stoker and Barker, 2020). These side effects, in combination with non-motor PD symptoms, present a significant negative impact on the patient's quality of life. In fact, it is often the non-motor symptoms that pose the greatest threat to a patient's quality of life and functional independence; yet, there are limited treatment options available for these symptoms. Currently, the most effective therapeutic for the treatment of PD is L-dopa, which was first developed in the 1960's (Stoker and Barker, 2020; Hornykiewicz and Birkmeyer, 1961). L-dopa reduces motor symptoms through increased dopamine levels in the striatum. Since this development, other dopaminergic therapies have been discovered and used in the treatment of PD. However, none of these approaches have revealed a disease-modifying effect. Thus, there is an urgent need for better treatments, but multiple barriers exist. For instance, there is paucity of accurate, pre-clinical disease models for testing purposes, and a lack of biomarkers for diagnosis (Stoker and Barker, 2020). Currently, medical research has progressively moved from dopaminergic drug discovery to advances in targeted therapies and biomarker development, with a goal to both increase patient quality of life and halt/reverse disease progression (Ntetsika, Papathoma and Markaki, 2020; Stoker and Barker, 2020).

Etiology of Parkinson disease

The etiology of PD is still incompletely understood and largely unknown. There remains a consensus that environmental factors such as multiple head traumas, rural living, farm life, and

exposure to well water increase one's risk of developing PD; however, the main initiating events are still undetermined (Kouli, Torsney and Kuan, 2018). It is believed that a combination of environmental factors and genetic susceptibilities could be the cause of initiation (Tomlinson *et al*. 2017). One hypothesis suggests that a main environmental trigger is microbial in nature – that is, bacterial pathogens and viral infections could initiate disease onset, whether it being primary, typical (sporadic) Parkinson's or secondary parkinsonism. The latter hypothesis arose following the influenza pandemic after 1918, where researchers noticed a sudden increase in the incidence of PD (Martyn and Osmond, 1995; Braak *et al,* 2003).

Influenza is a highly contagious virus that causes infection of the upper and lower respiratory tracts in humans. Infections can range from mild to severe and can sometimes be fatal. In some patients, complications within the central nervous system occurs as a result of systemic infection. Following the 1918 pandemic of the H1N1 Influenza variant, increased incidents of PD or parkinsonism were observed. It was reported that people born during the time of the pandemic had a 2-3-fold increased risk of developing PD compared to people born in the decades prior to or after 1918 (Martyn and Osmond, 1995). This statistic initiated the viral parkinsonism hypothesis (put forth first by Constantin von Economo), proposing that microbial infections may be an environmental trigger of PD. One study published by Cocoros *et al* (2021) further examined if influenza infections could be associated with PD. Using data from the Danish National Patient Registry, they identified that influenza diagnoses from 10 years prior were associated with a higher risk of PD. Of note, while this study shows the association between influenza and PD, it does not demonstrate direct causality (Cocoros *et al,* 2021). While the hypothesis remains controversial, evidence supporting it has undoubtably been accumulating. Linkage between parkinsonism and other viral infections have since been identified. Some

viruses include West Nile virus (WNV), human immunodeficiency virus (HIV), herpes simplex virus, Japanese encephalitis virus (JEV), and Epstein-Barr virus (EBV) (Leta *et al,* 2022). It is thought that exposure to such viruses can initiate parkinsonism through immediate cellular damage (para-infections) or delayed damage of mechanisms (post-infections) and that continued/repeated infections could lead to the worsening of neurological complications (Leta *et al*, 2022).

Genetic factors contributing to the onset of PD are also extensively being researched. The first gene identified with linkage to PD was *SNCA*. *SNCA* encodes the protein alpha-synuclein (aSyn), which is largely observed in PD patient brains in the form of insoluble cytoplasmic inclusions. Beyond genetic forms of *SNCA*-linked PD (which are rare), the presence of these aSyn-rich inclusions, termed Lewy bodies, are considered the pathological hallmark of typical, late-onset sporadic Parkinson disease. While the majority of sporadic PD cases are not associated with mutated aSyn, some familial forms of PD associated with specific aSyn mutations do exist. Several different point mutations within the protein sequence have been identified in PD patients, namely A53T, E46K, A30P, G51D, H50Q, and V15A. Additionally, allelic multiplication events have been observed in patients with heritable disease and have shown to increase one's risk of developing PD in an allele dose-dependent manner (Hernandez *et al*, 2021). Since the discovery of *SNCA*, additional genes associated with PD have been identified. Mutations in *GBA1* and Leucine Rich Repeat Kinase 2 (*LRRK2*) are considered to be common causes for dominantly inherited PD, while mutations in *PRKN* and *PINK1* are thought to be the commonest cause of autosomal recessive PD (Klein and Westenberger, 2012).

Disease pathology and pathogenesis

Synucleinopathies encompass a group of disorders including PD, dementia with Lewy bodies (DLB), and multiple system atrophy (MSA). These synucleinopathies are classified by abnormally misfolded aSyn aggregates in neurons/glia, presenting in the form of cytoplasmic inclusions known as Lewy bodies/Lewy neurites (Coon and Singer, 2020; Koga *et al*, 2021). These cytoplasmic inclusions are hence considered a major pathological hallmark of PD. Lewy bodies received their name after Friedrich Lewy, who first described cytoplasmic inclusions in 1923 following the study of PD patients (some presenting with symptoms of dementia) (Coon and Singer, 2020). Lewy bodies can further be classified into two types: classical/brainstem and cortical. While classical Lewy bodies appear as round, eosinophilic inclusions, cortical Lewy bodies are less compact/structured and are therefore more difficult to detect (Koga *et al*, 2021). Both types, however, can be found present within PD patients and always contain aggregates of insoluble aSyn. Yet, it remains unclear how aSyn aggregates and forms these Lewy body structures.

As discussed, non-motor symptoms of PD are thought to exist up to decades prior to motor manifestation of the disease (prodromal period). It is hypothesized that the pathological processes observed in PD may already be underway at this point. In fact, symptoms of prodromal PD (i.e. constipation, impaired olfaction, and sleep disorders) suggests that other areas of the body, aside from the brain, are implemented in PD pathology. This influenced the idea behind the dual-hit hypothesis, also known as the Braak hypothesis, where PD pathology essentially beings in both the gut and the nasal cavity then proceeds to spread in specific patterns through the vagal nerve and olfactory tract towards the central nervous system (CNS) (Rietdijk *et al*, 2017).

To address this spreading pattern, Braak and colleagues proposed a staging scheme. They declared that the earliest stage of PD (stage 1) could be characterized by the detection of aSyn aggregation within the olfactory bulb or medulla oblongata, and that clinical parkinsonism (i.e. motor-symptoms) and neuronal loss occurs later in the disease course (Burke *et al*, 2009). Following disease onset in the gut and nasal cavity, they proposed that disease progression spreads, travelling via axonal bundles of the vagus nerve to the medulla and the anterior olfactory nucleus into the brainstem (stage 2). After infiltrating the brainstem, Braak *et al* proposed that aSyn pathology begins to enter the *Substantia nigra* (stage 3) where the typical Lewy bodies form and the first clinical motor manifestations of PD arise from. They further suggest that following inclusions of the midbrain, cell degeneration ensues in the limbic regions (i.e. pars compacta, hypothalamus, thalamus, and mesocortex) (stage 4) and Lewy body inclusion formation advances to neocortical areas within the brain (stage 5), where eventually the majority of the neocortex will be affected, resulting in severe cognitive decline (stage 6) (Koga *et al*, 2021). This staging model for PD has since influenced the targets of PD research, especially in the field of biomarkers/targeted therapies. However, how aSyn pathology moves between regions is still up for debate. Currently, the commonest theory put forth is that aSyn acts as a prion protein and undergoes prion-like propagation from cell-to-cell.

The prion hypothesis

The theory that aSyn undergoes prion-like spreading first originated in 2003 where aSyn aggregation was observed within grafted fetal mesencephalic progenitor neurons, apparently after an average of 14 years following transplantation (Jan *et al*, 2021). Prions are infectious agents in which the altered/misfolded protein corrupts normal surrounding proteins, in turn creating a self-propagating species of misfolded protein which can spread between cells (Jan *et*

al, 2021). Additional proteins associated with neurodegenerative diseases such as beta-amyloid, tau, and Huntingtin, have also been speculated to undergo this prion-like spreading. Yet, the hypothesis still leaves cause for skepticism and remains a topic of debate amongst researchers.

Evidence supporting the prion-like spreading of aSyn has grown. In rodent models, inoculation of aSyn pre-formed fibrils via intracerebral injections resulted in widespread Lewy body-like inclusions (Chen and Mor, 2023) . Additionally, it has been shown that aSyn pathology is able to spread to the central nervous system of rodents following the injection of aSyn aggregates in various sites, including intravenous, intramuscular, and intraperitoneal (Chen and Mor, 2023). The prion hypothesis of aSyn was supported by evidence pointing at gut-to-brain transmission. Injections of human aSyn fibrils into the intestinal wall of rodents resulted in aSyn accumulation within the vagal nerve within 2 days post-inoculation (Holmqvist *et al*, 2014). In addition to rodent models, *Caenorhabditis elegans* models have also shown cell-to-cell transmission of aSyn. It has been demonstrated that aSyn travels from neuron to neuron, but more importantly, it can travel back/forth between neurons and pharyngeal muscle cells (Chen and Mor, 2023). The transmission of aSyn between neurons and muscle cells has also been associated with increased neurodegeneration and decreased survival/function, bringing forth the assumption that aSyn transmission causes increased toxicity (Chen and Mor, 2023).

Despite the accumulating evidence in support of the prion-like propagation of aSyn, some researchers are still skeptical of the hypothesis. The likely major cause for skepticism lies behind the lack of aSyn pathology within both the enteric nervous system (ENS) and CNS of ‘healthy’ individuals. It can be argued that if aSyn pathology begins in the gut, seemingly healthy individuals with undiagnosed/prodromal PD should contain aSyn pathology in the ENS or vagal nerve, but not yet in the CNS (Chen and Mor, 2023). Such cases could be described as Incidental

Lewy body disease (ILBD), where Lewy bodies are present in autopsied individuals that lacked clinical features of and were not diagnosed with PD or dementia (Adler *et al,* 2010). Thus, alternative hypotheses have been debated.

In an effort to appeal to both argumentative sides, some suggest that incidents of PD fall into two contrasting categories that can be based on the route of aSyn spread. One category is classified as brain-first PD. This involves the theory that aSyn pathology begins in the brain within the olfactory bulb or amygdala, and then spreads to the ENS via the vagal nerve. Specifically, aSyn pathology could spread from the amygdala through afferents (nucleus tractus solitarius) connecting it to the vagal nerve, then subsequently descend from the vagal nerve through to the esophageal hiatus allowing pathology to reach the abdominal cavity. The second category is classified as body-first PD, which suggests that aSyn pathology first exists within the ENS, and subsequently spreads to the CNS via the vagal nerve (Chen and Mor, 2023). Clinical evidence and studies conducted in animal models suggest that aSyn can travel bidirectionally and supports this dual trajectory hypothesis. Thus, it is likely that PD can be classified into multiple subtypes. If so, understanding these subtypes and generating a clearer definition of PD would greatly impact the future of targeted treatments, and in turn overall patient diagnosis/health.

Alpha-Synuclein

While the formation of aSyn-rich Lewy bodies can be considered one of the major hallmarks of PD, the natural function/role of the protein has yet to be fully characterized. It is thought that aSyn plays a role within the synapse, contributing to modulating neurotransmission and overall synaptic function. Found in multiple cell types (including all neuronal cells and in blood cells), aSyn exists predominantly within the pre-synaptic terminals in healthy individuals (Bisi *et al,* 2021). In PD patients, the protein often becomes mislocalized as aggregates within

the cytoplasm or its level rises in the nucleus. The mislocalization of aSyn is hence thought to be a disease-contributing factor, yet the mechanisms that allow this event to occur remains largely unknown (Miraglia *et al,* 2018).

Protein structure and properties

aSyn is a small, 140 amino acid protein product of the gene *SNCA*, which is located on the long arm of chromosome 4 (Villar-Piqué, Lopes da Fonseca and Outeiro, 2015). The primary sequence of aSyn is divided into three domains: the N-terminal, amyloid-binding central domain (NAC), and C-terminal domain (Villar-Piqué, Lopes da Fonseca and Outeiro, 2015). The N-terminal is positively charged and contains seven lipid-binding 11-residue repeats allowing the protein to undergo lipid binding and take the form of an alpha-helix structure. The NAC region is considered the core region of the protein. By forming cross beta-structures, the NAC is largely involved with fibril formation and aggregation (Emamzadeh, 2016). While the N-terminal and NAC domains are quite structured, the opposite is true for the C-terminal domain. The unstructured form of the C-terminal domain is due to its negative charge and low hydrophobicity (Emamzadeh, 2016). Of note, this domain is acidic, glutamate-rich, involved in many protein interactions, and is prone to various post-translational modifications (PTMs). The interaction between the C-terminal and NAC domain provides the ability to protect the protein from forming aggregates. (Burre, Sharma and Sudhof, 2018; Emamzadeh, 2016). There exists a theory that a vital component to this inhibitory effect is the phosphorylation of serine 129 (pS129). Therefore, mutations obstructing this phosphorylation site (including residue substitutions and truncations) are thought to cause aSyn aggregation, and possibly contribute to PD pathology (Emamzadeh, 2016). However, over 90% of aSyn found within Lewy bodies is phosphorylated at serine 129.

Therefore, the true effect of this modification on the protein's ability to form aggregates still remains a debate.

In addition to aSyn, there are two other proteins in the synuclein family: beta-synuclein and gamma-synuclein. Of the members, beta-synuclein's expression is the most brain-specific with its expression restricted to neurons, while gamma-synuclein is least expressed in the brain. However, they both localize to synaptic terminals, similar to aSyn, and overlap with aSyn expression in specific areas of the brain (Burré, 2015). It is notable that beta and gamma-synuclein are absent from Lewy bodies; however, in PD they co-localize with aSyn in spheroid-like neuronal inclusions and it is suggested that they may be involved in neurodegenerative diseases, including PD. (Burré, 2015; Villar-Piqué, Lopes da Fonseca and Outeiro, 2015).

Mutations in alpha-synuclein

To date, many mutations of aSyn have been documented and are suspected to be associated with familial forms of synucleinopathies. Single point mutations within the N-terminal domain are the most widely studied in scientific literature; namely A53T, E46K, A30P, and G51D. Some of these mutations (A53T, E46K) have been linked to early-onset forms of PD (Gardai *et al,* 2013; Perni *et al,* 2021). It has been observed that many of these mutations have an increased propensity to form aggregates (i.e. A53T and E46K), an increased propensity to form fibrils (i.e. A53T and G51D), can reduce lipid binding (i.e. A30P and G51D), are prone to form oligomers (i.e. A30P), and can impair autophagy (A30P) (Gardai *et al,* 2013; Perni *et al,* 2021; Ruf *et al,* 2019; Lei, Cao and Wei, 2019; Villar-Piqué, Lopes da Fonseca and Outeiro, 2015).

In addition to several PD-linked point mutations, additional aSyn mutations have been developed for their use as research tools to better understand aSyn function and biology. Located in the C-terminal domain, the S129A mutation specifically prevents phosphorylation at serine

129 and has been linked with increased toxicity (Azeredo da Silveira *et al*, 2009). The phosphorylation of serine 129 is thought to contribute to aSyn induced toxicity, largely due to the majority of aSyn species within Lewy bodies are phosphorylated at this site. Thus, removing the ability of aSyn to undergo phosphorylation at this site could prove a useful tool in further understanding disease pathogenesis. It should be noted, however, that recent studies suggest that the phosphorylation of S129A could also act as a regulator for neuronal activity (Ramalingam *et al,* 2023). In addition to this, Hernandez *et al* (2021) also described a C-terminal deletion of 21 amino acids beginning at amino acid 119 (d119). Of note, C-terminal truncated forms of aSyn have been found in PD patient brain autopsies and are thought to induce fibril formation and cell toxicity (Zhang *et al,* 2022). Still, little is known about the underlying mechanisms of truncated aSyn species and how they may contribute to aSyn aggregation and Lewy body formation (Zhang *et al,* 2022). Additionally, the C-terminal is largely unstructured in aSyn, allowing it to be a good target for PTMs. In effect, d119 favors fibril formations through its ability to cause mechanistic changes of lipid-induced aggregation and amyloid function. As well, by removing the common phosphorylation site (serine 129), this truncated form of aSyn could aid in the understanding of disease pathogenesis/progression. In the same study, Hernandez *et al* (2021) also documented a triple-point alanine to proline mutated aSyn at amino acids 30, 56 and 76 (3xA-P). Their study shows that by substituting the alanine acids to proline at these sites, the protein is more able to undergo oligomerization (Hernandez *et al,* 2021). The formation of multimers (i.e. tetramers), however, have been described as normal part of aSyn metabolism to prevent aggregation (Bartels, Choi and Selkoe, 2011). In their paper, Bartels, Choi and Selkoe identified that endogenous aSyn from various cell lines and tissues occurred predominantly as folded tetramers, and was not purely monomeric as previously suggested.

Physiological functions of alpha-synuclein

While the study of aSyn has been ongoing for over 30 years, the typical function of the protein remains largely unknown. Determining the normal function of aSyn has proven challenging, likely in part because of the protein's unstructured formation as well as its tendency to overexpress and trigger toxic effects (Burré, 2015). However, within the brain, many studies have suggested that it may be involved in regulatory functions of the synapse. Such functions include synaptic activity/plasticity, modulating synaptic transmission and stress responses, neurotransmission, vesicle trafficking/recycling, membrane cleavage, regulation of homeostasis, and dopamine metabolism (Waxman and Giasson, 2009; Burré, 2015; Kasen *et al*, 2022). However, the exact mechanisms relating to these functions remains undetermined. In addition, the absence of aSyn within other non-human species (*e.g.* worms, flies, and yeast) suggests that the protein is not *required* for such functions, and perhaps simply contributes to long-term operations (Burré, 2015). In fact, numerous studies have observed opposing results. For example, some record aSyn as promoting neurotransmission, while others report that aSyn inhibits or has zero effect on neurotransmission (Ramalingam *et al,* 2023).

While unresolved as of yet, the role of aSyn within neurons has been largely documented and studied. However, the protein's role in different cell types remain to be elucidated (Kasen *et al*, 2022). aSyn was first identified as a nuclear/presynaptic mammalian protein found in neurons. It is now understood that aSyn has some expression throughout the entire body, including within immune cells (Kasen *et al*, 2022). aSyn has been observed to interact with the SNARE complex through protein interactions (i.e. synaptobrevin-2) and chaperoning SNARE-complex assembly (Burré, 2015; Kasen *et al*, 2022; Tan *et al*, 2022). SNAREs have been characterized in various immune cells with various different functions relating to phagocytosis

and receptor recycling (Kasen *et al*, 2022). When acting as a chaperone (i.e. assisting in protein folding) aSyn has been speculated to aid in the prevention of aggregate formation, likely via the C-terminal domain's ability to bind to the synaptic vesicle (Kasen *et al*, 2022). Of note, changes in aSyn formation, including the increased formation of oligomers, can disrupt the SNARE complex and can also cause changes in dopamine levels and synaptic-vesicle release (Kasen *et al*, 2022).

Aside from increased oligomerization, mutations and modifications of aSyn may negatively affect its typical function. Few studies have suggested that post-translational modifications and specific point mutations block the protein's natural abilities and influences the creation of fibrils and aggregates (Tan *et al*, 2022). It has been suggested that such changes can induce cellular stress responses which ultimately result in neurodegeneration (Kasen *et al*, 2022). Additionally, the disruption of SNARE complexes may also have dire consequences on the immune system through alterations in immune cell signalling (Kasen *et al*, 2022). As mentioned, aSyn has been found to exist within immune cells (i.e. hematopoietic cells including T and B cells, monocytes, and natural killer cells) (Shin *et al,* 2000). Such implications within the immune system have led to the study of aSyn and its possible role(s) during pathological viral/bacterial invasions. To date, no studies seem to definitively demonstrate that microbial infections directly cause PD; however, some do show that such infections can lead to aSyn production/alterations (Kasen *et al*, 2022). Whether the overproduction/changes observed in aSyn are a response to infections via host defence or a consequence thereof remains unknown.

PD and the Innate Immune System

While the etiology of PD still remains quite elusive, general consensus amongst researchers details a combination of genetic and environmental triggers. Many different

environmental factors have been studied for potential disease-initiating properties. Currently gaining popular interest is the hypothesis for microbial infections to exhibit such properties. To date, there has been ample evidence to support immune system involvement in the development of PD. Observations of increased incidents of parkinsonism following select viral outbreaks is perhaps the main contributing factor to this hypothesis. In fact, the origin of this hypothesis can largely be contributed to the H1N1 Influenza pandemic of 1918, with linkage to the encephalitis lethargica outbreak (Leta *et al*, 2022; Smeyne *et al*, 2021). Briefly prior to the H1N1 pandemic, encephalitis began to spread across the globe. As described by von Economo in 1917, encephalitis was an epidemic neurological syndrome following influenza infection, and it has since been found to contribute to subsequent post-encephalitic parkinsonism (Leta *et al*, 2022).

Viral infections have been shown to induce parkinsonism in one of two fashions: para-infections and post-infections. Para-infections relate to a clinical event occurring within 15 days of initial infection onset. Viruses causing para-infections are usually neurotropic and directly able to damage the CNS (Leta *et al*, 2022). In contrast, post-infections relate to a clinical event occurring months-decades after the initiating infection. As such, post-encephalitic parkinsonism is believed to originate months-years following initial infection and occur via pathogen-induced autoimmunity (Leta *et al*, 2022). It has been estimated that up to 50% of PD cases were post-encephalitic in the decades following the outbreak, raising suspicions for the hypothesis that PD can stem from microbial infections (Leta *et al*, 2022).

As mentioned previously, observations of PD were higher in the years following the H1N1 influenza pandemic, with evidence that people born during the pandemic had a higher risk of developing PD compared to those born in the decades prior to or after the outbreak (Smeyne *et al*, 2021; Jang *et al*, 2015) and that infection even ten years prior (i.e. possible prodromal

period) could increase one's likelihood of developing PD (Cocoros *et al,* 2021). This prodromal period makes measurements of initiating factors challenging and can attribute to the hardships of early-onset diagnoses and the establishment of definitive causation of Influenza infections (Smeyne *et al*, 2021).

Aside from the 1918 H1N1 influenza variant, additional strains are thought to induce parkinsonism in an analogous manner. Variants such as H1N1, H2N2 and H3N2 are considered non-neurotropic, and are suggested to contribute to post-infectious encephalitis/parkinsonism despite the lack of direct damage/infection of the CNS (Smeyne *et al*, 2021). These different variants share the ability to cause systemic infections. During infection, increased levels of cytokines and chemokines are produced, which are then able to pass through the blood brain barrier (Smeyne *et al*, 2021). Some cytokines (i.e. TGFalpha, IL6, IFNg) which are upregulated during Influenza infections have been shown to induce inflammatory responses within the brain, leading to neuronal cell dysfunction/death. These findings suggest that inflammation stemming from viral infections may make the CNS more susceptible for later insult, which is perhaps what occurred during post-encephalitic parkinsonism development following the 1918 pandemic (Smeyne *et al*, 2021). Following the initial damage occurring as a result of infection, it is hypothesized that persistent infections may continued to derive immune responses and neuronal damage. Of note, additional viruses have been documented as potential PD triggers including human immunodeficiency virus (HIV), Hepatitis B, and Hepatitis C (Leta *et al*, 2022; Smeyne *et al*, 2021).

As mentioned previously, olfactory impairment is one of the most common symptoms of prodromal PD. Following the Braak staging hypothesis, the role of infection as an environmental trigger gains even more plausibility. With the above in mind, speculations of Severe Acute

Respiratory Syndrome Coronavirus 2 (SARS-CoV-2) in the aided development of PD are on the rise. SARS-CoV-2 (causing Covid-19) is a respiratory virus responsible for the latest pandemic, spanning across nearly three years. Olfactory impairment via (albeit transient) loss of smell is one of the common symptoms of the disease. Given the evidence supporting viral infection-induced parkinsonism and the similarities of olfactory symptoms between SARS-CoV-2 and PD, researchers are currently investigating the possible linkage of olfactory impairment to neurodegeneration (Emmi *et al*, 2022). Viral infections, however, are not the only pathogen to raise concern. It has been suggested that bacterial strains (such as *Staphylococcus aureus)* capable of inducing inflammatory responses within the olfactory system may also trigger neurodegeneration and protein aggregation (Emmi *et al*, 2022; Murros, 2022). Furthermore, bacterial pathogens are speculated to induce infection within the gut, possibly inducing systemic infections leading to parkinsonism. For instance, bacterial species within the gut microbiome of PD patients have shown to produce larger amounts of hydrogen sulfide (H_2S). When produced in excessive amounts, H_2S can lead to the formation of aSyn aggregates, oligomers, and fibrils via the release of cytochrome c protein and increased reactive oxygen species (ROS) production (Murros, 2022). Therefore, it is speculated that gut bacteria responsible for producing increased H_2S are likely to play a role in PD pathogenesis. It is further hypothesized that influenza infections could increase the risk of developing PD by initiating the overgrowth of bacteria in the gut which produces H_2S (Murros, 2022). While it still remains open for discussion, the evidence to support microbial infections – whether bacterial or viral – as environmental triggers of PD are undoubtedly piling up. Still, the mechanisms contributing to PD pathology, such as the formation of aSyn-rich Lewy bodies, are undetermined.

Alpha-synuclein as an immune protein

As previously noted, the formation of aSyn-rich Lewy bodies is considered to be a pathological hallmark of PD. (If, and) How microbial infections might lead to the altercations observed in the protein remains undetermined. A hypothesis exists where aSyn plays a natural, protective role within the innate immune system, and that altercations in its metabolism following select microbial infections could lead to the disease initiating events as seen in PD. To date, various models have been utilized to study the possible cyto-protective qualities of aSyn against both bacterial and viral infections.

PD patient autopsies have shown that aSyn deposits are located, not solely in the brain, but in the enteric nervous system and the gastrointestinal tract (Huynh *et al*, 2023). In accordance with the Braak staging of PD, it is possible that aSyn aggregation begins in the gut/olfactory bulb and moves towards the brain/CNS via the vagal nerve. Therefore, many studies have examined different pathogenic bacteria strains affecting these regions and their effect on aSyn. In contrast, some have studied the effect of aSyn on the pathogenic bacteria. A study conducted by Park *et al* (2016) looked to identify possible protective qualities of aSyn against two pathogenic bacterial strains (*Escherichia coli* and *Staphylococcus aureus*) effecting the gastrointestinal and olfactory systems, respectively. They demonstrated that increasing concentrations of human endogenous aSyn produced increasing antibacterial effects by inhibiting bacterial growth in both tested strains (Park *et al*, 2016).

Similarly, our laboratory has previously demonstrated protective qualities of aSyn in mice against the pathogenic bacteria *Salmonella typhimurium*. It was found that mice with intact *Snca* (and thus able to produce aSyn) were able to more effectively control bacterial growth than mice that lacked *Snca (*and thus unable to produce aSyn) (Tomlinson *et al*, 2017). Evidence, such as

the presented, seems to indicate that aSyn acts within the immune system against harmful bacteria. However, whether and, if so, how aSyn transitions from a protective protein to a pathological/aggregate-forming protein is yet to be determined.

As discussed prior, H_2S producing bacteria have been studied for their involvement in PD-onset and aSyn aggregation. In a recent study presented by Huynh *et al* (2023), H_2S producing *Desulfovibrio* bacteria strains isolated from human PD patient samples were capable of producing more and larger aSyn aggregates than *Desulfovibrio* bacteria strains isolated from healthy human controls (Huynh *et al*, 2023). Additionally, they observed that *Caenorhabditis elegans* that were fed PD-patient *Desulfovibrio* bacteria had increased fatality rates than worms that were fed the control bacteria, which they attribute to likely being from the over-abundance of aSyn aggregates. How and why the protein becomes more pathogenic is yet to be determined; however, the answer may lie behind different strains of bacteria altering the protein's metabolism. Genome sequencing of these bacterial strains could shed light on this hypothesis and should be considered as a next step for researchers (Huynh *et al*, 2023).

Possible cyto-protective properties of aSyn have also been greatly studied against viral infections across many different experimental models. Complementary to their findings in bacterial studies, Tomlinson *et al* (2017) evaluated the ability for aSyn to protect mice against reovirus-TD3-induced infections. Reovirus-TD3 is a neurotropic respiratory-enteric-orphan virus known to cause brain infections in young mice, often leading to fatality. When administering the virus via the nasal pathway, systemic infection is initiated through the respiratory/intestinal tracts towards the brain (Tomlinson *et al*, 2017). Results indicated a correlation between decreased aSyn expression and decreased survival, demonstrating that endogenous aSyn may play a role in immune function to protect the mice from the reovirus infection (Tomlinson *et al*, 2017). Another

study published by Beatman *et al* (2016) provided evidence supporting an anti-viral for aSyn. In their study, aSyn was able to restrict infection of several RNA viruses (i.e. WNV and VEEV) in neuronal cell models and mouse models.

While the above evidence sheds light on possible protective qualities of endogenous, wild-type aSyn, similar evidence is needed to address variant forms of aSyn linked to familial-PD. Using transgenic mouse models, Hernandez *et al* (2021) evaluated mutations on the C-terminal domain, including a c-terminal deletion at amino acid 119 (d119) and a triple point alanine-proline mutation (amino acids 30, 56 and 76). Of note, these mice did not overexpress the mutated forms of aSyn but expressed them at similar levels to that of endogenous aSyn. While no dopaminergic neuronal loss was observed, impaired olfaction and motor deficits were noticed to similar extents in the mutant mice. Additionally, there was no evidence of altered pro-inflammatory cytokines; however, anti-inflammatory cytokines and chemokines were significantly up-regulated (Hernandaz *et al*, 2021). While their study shows that these mutated forms of aSyn produce an altered immunoactive state, their results are not definitive as to whether the altered response is neurotoxic or neuroprotective or is at all involved in a possible anti-microbial role for this protein. Analysis of mutations within the N-terminal of aSyn have also been studied for their possible involvement in host immunity. In a cell-based model, Gardai *et al* (2013) evaluated the effects of three different mutated forms of aSyn considered to be pathogenic and aggregate-prone, namely A53T, E46K and A30P. Through their analysis using transiently transfected human neuronal cell lines that express endogenous aSyn (H4 cells) they demonstrated that wild-type aSyn and all three mutated forms of aSyn could significantly block phagocytosis of latex beads compared to a vector-only control (Gardai *et al*, 2013).

Overall, the evidence supporting a cytoprotective role of aSyn within the innate immune response has gained great support and interest, yet, controversy remains. If continuing evidence suggests that aSyn does function as an immune protein, how it gets from a protective to a pathogenic state will need to be determined.

VSV model for Parkinson disease: rationale and pathogenesis

The purpose of the current study is to better understand the role(s) aSyn may play in innate host defense, and to characterize potential alterations of aSyn within the immune system and how microbial events may contribute to said alterations. Considering the linkage of microbial infections to PD still remains a debate, our lab sought to model a natural course of infection with relevance to previous studies through the use of a Vesicular Stomatitis Virus (VSV). VSV is a neurotropic virus capable of causing systemic infections in select animal hosts, such as rodents and cattle. Given the relevance of other neurotropic viruses' link to PD incidence, we have decided to implement this model to assess the immune involvement of aSyn in the context of infections.

VSV is an enveloped, single-stranded RNA virus inflicting disease in livestock via *Vesiculoviruses*. Enveloped viruses are often more sensitive to external stimuli/conditions largely due to their outer lipid bilayer, which contains receptors capable of recognizing host cells (Rousso, 2019). What is known collectively as VSV can be broken down into two serotypes: New Jersey and Indiana (Pelzel-McCluskey *et al*, 2021). Of note, our lab conducts its studies using the Indiana serotype wild-type VSV. Clinical manifestations of the disease in livestock include lesions on the lips, nostrils, inner-mouth, ears, and abdomen (Pelzel-McCluskey *et al*, 2021). While it typically directly infects livestock, VSV is considered zoonotic and can pass from livestock animals to humans. Infections in humans often lead to flu-like symptoms such as

fever, headaches, and fatigue (Pelzel-McCluskey *et al*, 2021). Given the implications of flu-causing viruses (*e.g*. H1N1) in PD and PD-associated events (i.e. the formation of aSyn aggregates), we believe that VSV is an ideal model virus to study the possible effects aSyn may have on host immunity (i.e. viral replication), as well as the potential effects that infectivity may have on the protein itself.

Our lab hypothesizes that aSyn may play a natural role in innate host immunity of vertebrates, and that alterations in the protein's metabolism following select microbial infections could lead to pathological tissue changes that are observed in PD. The overall goal of this thesis was to test whether aSyn acts as an immune-responsive protein, and identify how different formations of aSyn, including some disease-linked mutations and other investigative mutations, may contribute to possible disease initiating events observed in PD.

The goals and hypothesis of the present study were informed by the implications of aSyn within the immune system of vertebrates, including its ability to harbour protective qualities against viral/bacterial infections, and additionally its seeding capabilities from the gastrointestinal/olfactory systems to the brain, contributing to the Braak staging hypothesis with linkage to the theory that microbial infections may be an environmental trigger of PD. If the results from my study bear fruit, important discoveries relating to the involvement of aSyn within the immune system could conclude a better understanding of the etiology of PD and could better inform future studies of the disease. Understanding more about aSyn biology, including differences amongst its known point mutants, could provide further evidence of possible familial-linked subtypes of PD and could hence better inform ongoing research relating to personalized and targeted therapies. In this study, the characterization of aSyn both upstream and downstream of microbial infections was addressed through the use of various cell models in an

attempt to test the hypothesis that aSyn acts as an immune-responsive protein against microbial infections, and that alterations in its metabolism following said infections may lead to the pathological changes as seen in PD. To address this hypothesis, the following aims are presented: 1) to observe the ability of aSyn – including differences between various mutations of aSyn – to influence viral infectivity within neuronal cells, and 2) to observe the consequences of aSyn metabolism following a viral infection.

Chapter 2. Materials and Methods

Cell cultures

H4 (human neuroglioma, ATCC HTB-148) cells were cultured in high glucose Dulbecco's modified Eagle's medium (Sigma, D6429) supplemented with 10% fetal bovine serum. PC12 (rat adrenal gland pheochromocytoma, ATCC CRL-1721) and PC12-C4 (stably transfected PC12 cell line for overexpression of aSyn) cells (provided by Dr. Christopher Rochet, Purdue University) were cultured in RPMI-1640 (Gibco, 11875-093) medium supplemented with 10% fetal bovine serum and 5% horse serum. L929 (immortalized mouse subcutaneous connective tissue cells, ATCC CRL-6364) cells were cultured in Eagle's minimum essential medium (Sigma Life Sciences, M2279-500ML) supplemented with 10% fetal bovine serum, L-glutamine, Gentamycin, and 2-Mercaptoethanol. All cell lines were incubated in a CO_2 humidified incubator at 37°C.

PC12 Tet-off aSyn system

PC12-C4 cells were stably transfected with pTRE2-hyg-6His-aSyn prior to the initiation of my studies withing the Dr. Schlossmacher laboratory, as described previously (Mirzaei *et al*, 2006). Cell culture medium was supplemented with 200ng/µl doxycycline for a minimum of five days to reduce the expression of aSyn.

Plasmid preparation and sequencing

pcDNA3.1 vectors encoding either nothing (empty control), wild-type, A53T mutated, or E46K mutated aSyn were transformed in Dh5α chemically competent cells and plated on LB agar plates supplemented with ampicillin, which were subsequently incubated overnight at 37°C. Bacterial colonies were picked from the agar plates the following day and inoculated in LB broth supplemented with ampicillin and subsequently incubated overnight at 37°C in a shaking

incubator. The cultures were lysed the following day to extract and purify the plasmid DNA via either the Wizard Plus SV Minipreps DNA Purification System as per the manufacturer protocol (Promega Corporation, A1330), or the PureYield Plasmid Maxiprep System as per the manufacturer protocol (Promega Corporation, A2393). The purity and concentration of the plasmid DNA was assessed using a NanoDrop spectrophotometer (Thermo Fisher Scientific, ND-2000). Plasmid DNA samples were sequenced by the DNA Sequencing Facility at the Ottawa Hospital Research Institute to verify the correct nucleotide sequence. All constructs were kept in nuclease-free H_2O and -20°C for long term storage.

pENTR vectors encoding variants of aSyn, such as its wild-type(-3xFlag), C-terminally truncated (+3xFlag), C-terminally truncated without a Flag-tag (-3xFlag), triple point A-P mutated (+3xFlag), or triple point A-P mutated without a Flag-tag (-3xFlag) forms, were ordered and obtained from Twist Bioscience. Through Gateway Cloning technologies, plasmids were cloned using the LR Clonase II Plus Enzyme Mix (Thermo Fisher Scientific, 12538120) into the empty pDEST vector. The resulting pDEST plasmids were then transformed into ccdb-sensitive chemically competent cells (DH5α) and propagated in LB broth supplemented with ampicillin and grown overnight to select for the appropriate destination (pDEST) plasmids. The cultures were lysed the following day to extract and purify the plasmid DNA via the Wizard Plus SV Minipreps DNA Purification System as per the manufacturer protocol (Promega Corporation, A1330), or the PureYield Plasmid Maxiprep System as per the manufacturer protocol (Promega Corporation, A2393). The purity and concentration of the plasmid DNA was assessed using a NanoDrop spectrophotometer (Thermo Fisher Scientific, ND-2000). Plasmid DNA samples were sequenced by the DNA Sequencing Facility at the Ottawa Hospital Research Institute to verify

the correct nucleotide sequence. All constructs were kept in nuclease-free H_2O and -20°C for long term storage.

pDEST vectors encoding either wild-type, A53T mutated, G51D mutated, S129A mutated, or A30P mutated aSyn each containing a 3xFlag were obtained from Dr. Max Rousseaux. Upon obtainment the plasmids were transformed upon in Dh5α chemically competent cells and plated on LB agar plates supplemented with ampicillin, which were subsequently incubated overnight at 37°C. Upon obtainment the plasmids were transformed upon in Dh5α chemically competent cells and plated on LB agar plates supplemented with ampicillin, which were subsequently incubated overnight at 37°C. In addition, an empty pDEST vector, also obtained from Dr. Max Rousseaux, was transformed in XL-10-Gold chemically competent cells and plated on agar plates supplemented with ampicillin and subsequently incubated overnight at 37°C. Bacterial colonies were picked from the agar plates the following day and inoculated in LB broth supplemented with either ampicillin or kanamycin, and subsequently incubated overnight at 37°C in a shaking incubator. The cultures were lysed the following day to extract and purify the plasmid DNA via the Wizard Plus SV Minipreps DNA Purification System as per the manufacturer protocol (Promega Corporation, A1330), or the PureYield Plasmid Maxiprep System as per the manufacturer protocol (Promega Corporation, A2393). The purity and concentration of the plasmid DNA was assessed using a NanoDrop spectrophotometer (Thermo Fisher Scientific, ND-2000). Plasmid DNA samples were sequenced by the DNA Sequencing Facility at the Ottawa Hospital Research Institute to verify the correct nucleotide sequence. All constructs were kept in nuclease-free H_2O and -20°C for long term storage.

In vitro transfections

H4 cells were trypsinized (Wisent Inc., 325-542-EL) as per standard protocol and counted manually using a haemocytometer. 200,000 cells/well were plated in a 12-well plate and incubated overnight in a CO2 humidified incubator at 37°C to achieve a confluency of 70-75% prior to transfection. Transfections were completed using a 1:3 ratio of Lipofectamine 2000 reagent (Invitrogen, 11668-019) to DNA, as per manufacturer protocols, in the presence of OptiMEM (Gibco, 11058-021). Culture medium was replaced the following day and subsequent experiments were performed.

In vitro infection of VSV-GFP

Wild-type Indiana serotype vesicular stomatitis virus stocks expressing GFP (VSV-GFP) were obtained from Dr. Jean-Simon Diallo. The viral titre of the VSV-GFP stocks were confirmed by plaque assays. All stocks were aliquoted in smaller volumes to prevent frequent freeze-thawing. VSV-GFP aliquots were further diluted upon experimental use in serum-free culture medium. Infections were performed through the addition of 100ul of viral suspension onto the cells. The cells were incubated for 30 minutes at 37°C in a CO_2 humidified incubator, with manual shaking after 15 minutes. 1000µl of culture medium containing serum was then added to each well of cells and the infection was cells were incubated for the desired infection duration. Note, the addition of the culture medium after the 30-minute incubation is considered the start of the infection period. Once the desired infection duration had concluded, the cells were either fixed with 4% PFA directly in the well for fluorescent microscopy, trypsinized and fixed with 4% PFA in an Eppendorf tube for Flow cytometry or harvested for protein extraction.

Fluorescent signal quantification

Infected cells were fixed with 4% PFA for 15 minutes to avoid cell death during the imaging process. After fixation cells were washed twice with PBS (Wisent Inc., 311-425-CL) and nuclei stained with NucBlue Fixed Cell Stain ReadyProbes (DAPI) as per the manufacturer protocol (Invitrogen, R37606) in PBS. Cells were washed three times with PBS and left in 250µl PBS for imaging. Using the EVOS FL Auto2 Widefield Inverted Microscope (Invitrogen, AMF7000) provided by the CBIA Core at the University of Ottawa, 25% of each well was captured using GFP, DAPI, and phase contract channels. All images were stitched together to form a single image, which was subsequently used for quantification through ImageJ software available through FIJI software. In ImageJ, images were converted to 8-bit and the threshold was set to select either stained nuclei (DAPI) or infected cells (GFP). The average GFP signal intensity was analyzed in each well using the 'analyse particles' function. The total amount of infected cells in each well was analyzed by creating binary images and comparing the total amount of counted cells in the GFP channel to that of the DAPI channel. After statistical analyses were performed, representative images were taken using a ZOE Cell Imager (Bio-Rad, 1450031).

Flow cytometry

Infected cells were trypsinized as per standard procedure and collected in a 1.5mL Eppendorf tube. Cells were centrifuged at 500xG for 5 minutes then resuspended in 0.5mL PBS. Cells were fixed by adding 0.5mL of 4% PFA (Thermo Fisher Scientific, 50-980-487) for 30 minutes. Note that PFA was purchased at a concentration of 16% and diluted for use. After fixation, cells were centrifuged for 15 minutes at 500xg then resuspended in PBS containing no BSA or protein. Cells were then counterstained for viability with the ZOMBIE NIR Fixable Viability Kit (Biolegend, 423105). Cells were again centrifuged for 15 minutes at 500xg and

resuspended in 0.5mL of 0.2% BSA in PBS supplemented with 1mM EDTA and 25mM HEPES. Flow cytometry analysis was then conducted by Dr. Vera Tang through the Flow Cytometry and Virometry core at the University of Ottawa.

Western blotting

Cell pellets were lysed in 1% Triton-X100 buffer containing protease and phosphatase inhibitors. Protein concentration from the lysates were determined using a bicinchoninic acid assay kits (BCA) (Thermo Fisher Scientific, 23227; 23209; 23223). 10µg of each protein sample was mixed with NuPAGE LDS Sample Buffer (Invitrogen, NP0007) supplemented with 2-Mercaptoethanol (Gibco, 21985-023) and additional lysis buffer to standardize the total volume of sample mix. Samples were then heated at 95°C for five minutes and electrophoresed under reducing conditions on a 10% SDS, 4-12% bis-tris (SDS-PAGE) gel (Invitrogen, NP0321BOX; NP0322BOX; NP0336BOX). Transfer of gels to a membrane was performed using the Powerblot system as per manufacturer protocols (Invitrogen, PB0012; PB0013). Membranes were crossed-linked with 0.4% PFA by heating in the microwave for 30 seconds to prevent protein detachment. A ponceau staining step was included prior to blocking to confirm equal loading of samples. All membranes were blocked using 5% skim milk in 1X phosphate buffered saline tween (PBST). Primary antibodies used include Syn-1 (BD Biosciences, 610787, 1:1000 dilution), VSV (grown in-lab by Dr. Earl Brown, 1:4000 dilution) and B-actin (Santa Cruz, SC-81178, 1:1000 dilution). Primary antibodies were left to incubate on the membrane overnight at 4°C with shaking. Membranes were rinsed with PBST prior to addition of secondary antibodies. The secondary antibodies used include ECL anti-mouse IgG (Millipore Sigma, NA931V, 1:10,000 dilution) and ECL anti-rabbit IgG (Millipore Sigma, NA934V, 1:10,000 dilution). All secondary antibodies were incubated on the membranes for one hour at room temperature with

shaking. Membranes were then further rinsed and imaged with SuperSignal West Femto Maximum Sensitivity Substrate (ECL) (Thermo Fisher Scientific, 34094) using the ChemiDoc MP imaging system (Bio-Rad, 12003154).

Live-cell imaging

Live-cell imaging of H4 cells transfected with BiSyn cDNA construct and infected with wild-type VSV was completed through the CBIA core at the University of Ottawa. Cells were transfected with 0.5µg of plasmid DNA expressing BiSyn 24 hours prior to infection with VSV. VSV infections were performed with a MOI of 3 or 5. Mock treated cells and infected cells were recorded over the course of 21 hours, with still images being captured every 15 minutes. Still images were combined to form time-lapse videos of the cells.

Statistical analysis

GraphPad Prism 6.0 software was utilized to determine the statistical significance of quantified data. One-way ANOVA tests were conducted to compare groups of data, and differences were deemed significant when a *p*-value was less than/equal to 0.05.

Chapter 3. Results

Optimization and troubleshooting of a H4 neuroglioma transfection model for the study of aSyn within cellular innate immunity

Previous studies performed in our lab have shown that wild-type (WT) aSyn possesses protective qualities against microbial infections in mouse models (Tomlinson *et al*, 2017). However, how the overexpression of aSyn aids in cell protection against pathogens still remains a debate amongst researchers (Rodriguez-Losada *et al*, 2020). In the present study, we aimed to further investigate the possible protective qualities of aSyn within cell models and evaluate how different PD-linked mutations-, and select post-translational modifications of aSyn, may affect such qualities. Further we aimed to then investigate what effects microbial infections may have on the protein itself. To begin my investigation, experiments were primarily conducted using H4 neuroglioma cells which endogenously express human aSyn. These cells were chosen partially due to their neuronal properties, high transfection efficiency, and due to preliminary findings that aSyn appeared to protect H4 cells from a viral infection, which informed my study goals. H4 cells were transiently transfected with various aSyn expressing constructs, then subsequently infected with VSV-GFP. VSV is an RNA virus and is known to cause systemic infections in mice; it is used in our lab to study PD-linked gene-environment interactions in mice and in cell culture models. aSyn-expressing plasmid DNA, or empty vector backbones (vector controls) were transiently transfected into H4 cells, 24 hours prior to infection. Initial optimization steps were taken to confirm the optimal VSV-GFP multiplicity of infection (MOI) to use for my experiments (**Figure 1**). The optimal MOI (0.1) was chosen based on the maximum GFP signal observed via fluorescent microscopy, while protecting cell viability after a 24-hour infection period.

Once the initial optimization steps were complete, each aSyn construct being studied within this project was tested for potential anti-viral properties. A summary of the constructs employed is shown in **Figure 2**. Of note, two separate vector backbones were utilized within this study for the following rationale: Constructs within the pDEST vector backbone either contained or lacked a triple-point flag (3xflag) (**Table** 1). This 3xflag is a 21-amino acid sequence that is in frame with the C-terminus of the protein; it can be used for protein detection using anti-Flag antibodies, for example. For the initial screening of each aSyn construct and vector control construct tested, H4 cells were transfected and subsequently infected with VSV-GFP (0.1 MOI) for 20 hours. Cells were fixed post-infection and GFP-signal was observed. Differences in infection efficiency were noted between the pcDNA3.1 and pDEST vector controls as measured by GFP-positive cells (**Figure 3**). The high level of GFP-signal observed in the cells transfected with the pcDNA3.1 vector control compared the minimal GFP-signal observed in the cells transfected with the pDEST vector control caused concern that the two vector types were non-comparable. Upon further investigation of differences in GFP-signal produced following infection with VSV-GFP, it was evident that the variability in detectable GFP-signal did not just exists between the vector types, but also within the same construct when experiments were replicated. For example, three experimental replicates using only the pcDNA3.1 vector control were performed and infected with VSV-GFP at either MOI 0.1 or MOI 0.5 (**Figure 4**). As shown, the GFP-signal observed from each infection remained inconsistent.

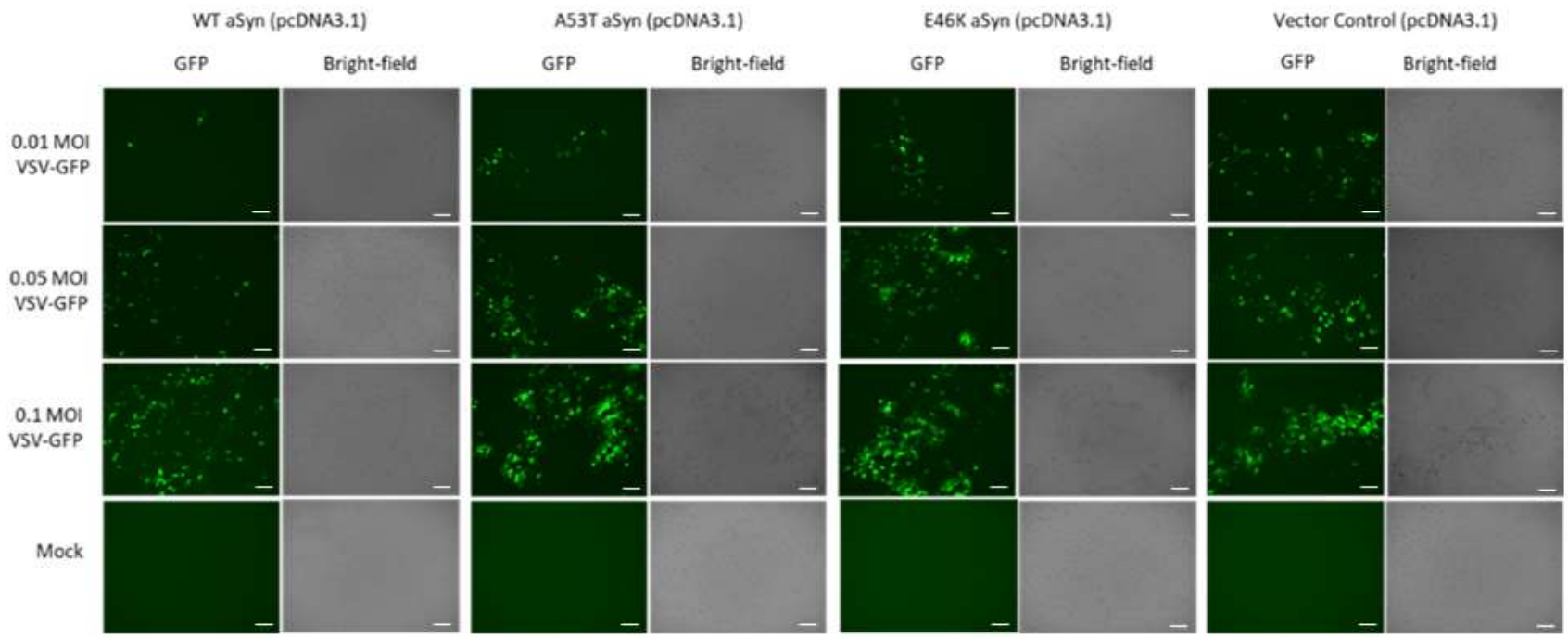

Fig 1. Optimization of VSV-GFP MOI to be used in H4 cell experiments. H4 cells transiently transfected with either WT or mutant aSyn were cultured in high glucose DMEM supplemented with 10% FBS and subsequently infected with VSV-GFP at increasing MOIs (MOI 0.01, 0.05, 0.1) for 24 hours. Fluorescent microscopy images (GFP, bright-field) were captured to assess the optimal MOI for maximum GFP-signal detection and maximum cell viability. Scale bar, length 100 microM.

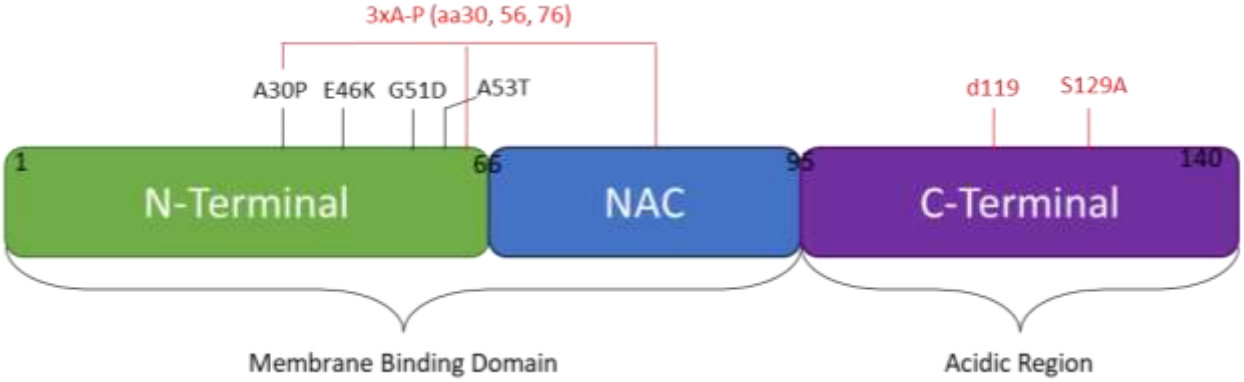

Fig 2. Alpha-synuclein protein structure. The structure of aSyn is visualized, including PD-linked mutations (black) and lab-created mutations (red) of aSyn which are employed in the present study.

Table 1. Summary of constructs used to transiently transfect H4 cells in the present study. Mutations/variations of aSyn are categorized based on their respective vector backbone.

pcDNA3.1 Constructs	pDEST (+3xFlag) Constructs	pDEST (-3xFlag) Constructs
Empty vector control	gSyn (gamma-syn)	Empty vector control
WT aSyn	WT aSyn	WT aSyn
A53T aSyn	A53T aSyn	A53T aSyn
E46K aSyn	A30P aSyn	d119 aSyn
	G51D aSyn	3xA-P aSyn
	S129A aSyn	
	d119 aSyn	
	3xA-P aSyn	

To combat the issue of inconsistency in the amount of GFP-signal produced post-infection several concrete troubleshooting steps were taken. A full list of steps can be found in **Appendix Table 1**. These included further optimization of VSV-GFP MOI used and the infection duration, optimization via protocol adaptations, and sequencing of each construct utilized within my project to ensure, in part, that the empty vector control plasmid was indeed empty. After taking these steps to eliminate the variability within the vector control samples, inconsistencies still persisted.

Next, it was hypothesized that contaminants within the plasmid DNA could be inducing an interferon response, thereby impairing the infectivity of the VSV-GFP virus. To address this theory, lipopolysaccharide (LPS) was used to treat untransfected cells prior to VSV-GFP infection (**Figure 5**). LPS is a bacterial toxin which should invoke an interferon response produced by the H4 host cells. In parallel, both the pcDNA3.1 vector control and pcDNA3.1 WT aSyn constructs were used to transfect cells that were not treated with LPS. Of note, a separate well of cells was treated with the transfection reagent, Lipofectamine2000 (L2000), without the addition of plasmid DNA as a control. From this, there was no evidence of altered GFP-signal production when the cells were pre-treated with increasing concentrations of LPS, and infection efficiency (as determined via GFP-signal) mimicked that of the L2000 control. Yet, GFP-signal (as a readout of viral infection) was greatly decreased in both the WT and vector control samples. This suggested that possible impurities in the plasmid DNA preparations, that could trigger IFN signalling, were not enough to affect the infection efficiency and that infection efficiency should not have been affected due to an interferon response.

After undergoing vigorous troubleshooting processes, a new theory of CMV promotor competition was suggested. During transcription, RNA and DNA polymerases are recruited to

the promoter of a gene. Promoter competition could come into effect due to the lack of a cDNA-based ‘foreign minigene’ to be transcribed within the vector control(s), meaning that the CMV promoter is ‘recruiting and binding’ polymerases in excess, thus rendering the VSV-GFP genome less able to recruit them and thus, replicate less efficiently.

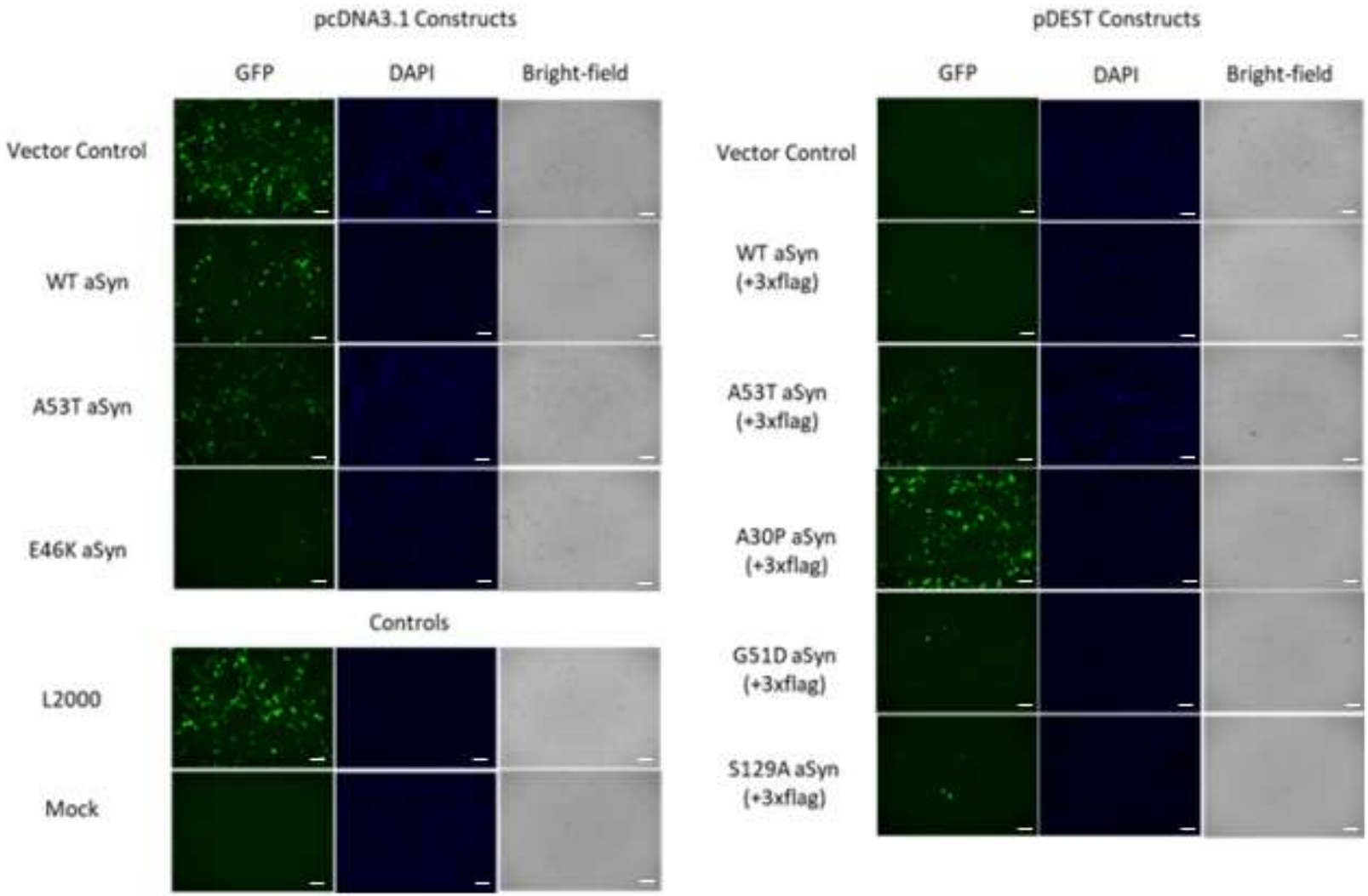

Fig 3. Initial screening of all aSyn constructs employed in the present study following VSV-GFP infection. H4 cells transiently transfected with either WT or mutant aSyn were cultured in high glucose DMEM supplemented with 10% FBS and subsequently infected with VSV-GFP (MOI 0.1) for 24 hours. Fluorescent microscopy images (GFP, bright-field) were captured to assess differences in GFP-signal following viral infection. Scale bars, length 100 microM.

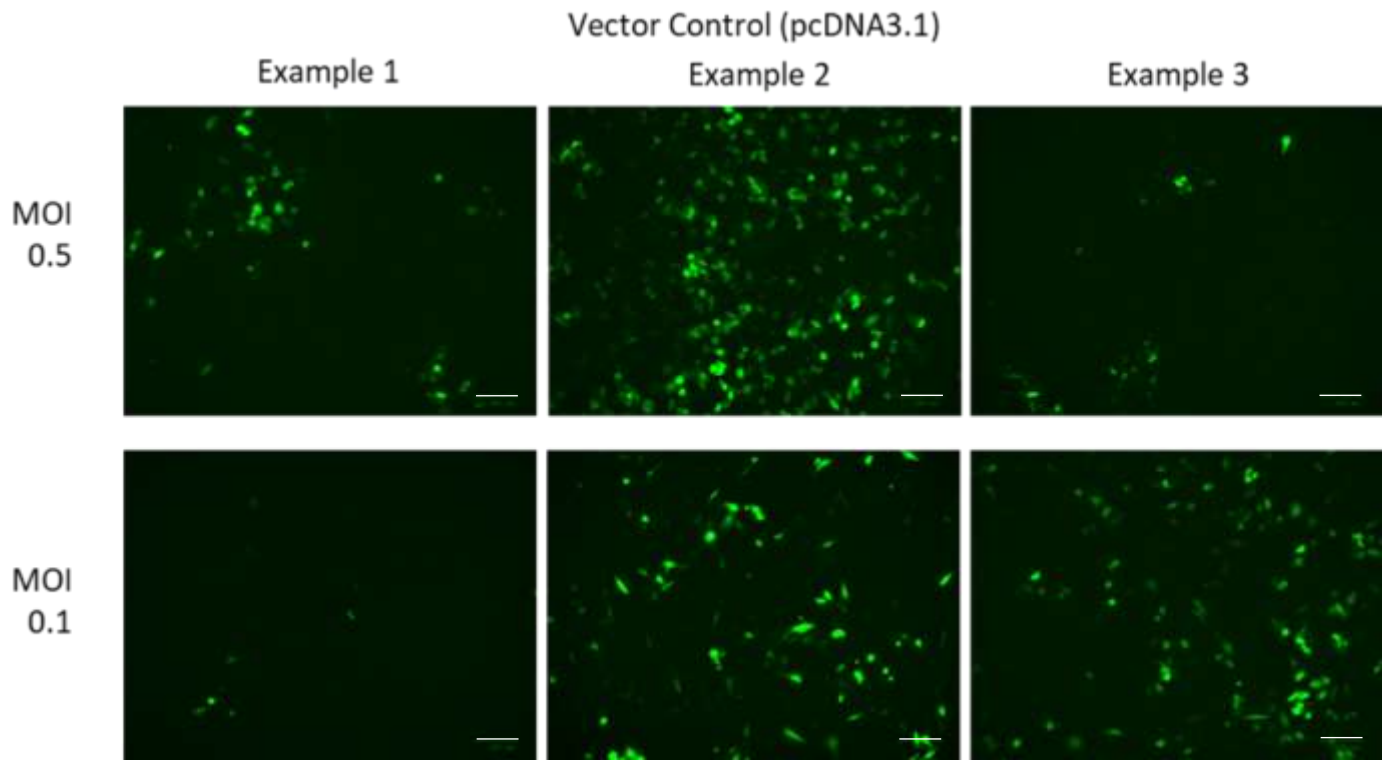

Fig 4. Fluorescent microscopy identifies large variability in GFP-signal production following VSV—GFP infection in H4 cells transiently transfected with the pcDNA3.1 vector control. H4 cells transiently transfected with the pcDNA3.1 empty vector control were cultured in high glucose DMEM supplemented with 10% FBS and subsequently infected with two MOIs of VSV-GFP (MOI 0.1, 0.5) for 24 hours. Three experimental replicates were performed. Fluorescent microscopy images (GFP, bright-field) were captured to assess differences in GFP-signal following viral infection and demonstrate variability in results produced by the vector control. Scale bars, length 100 microM.

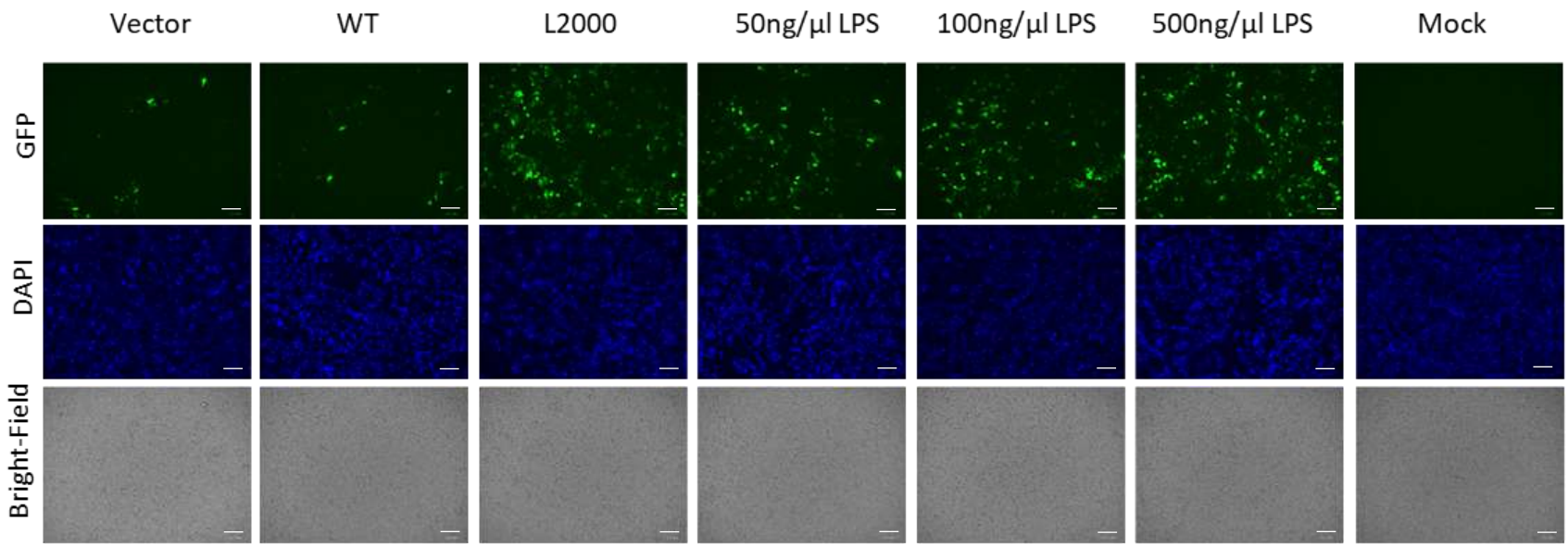

Fig 5. Treatment with LPS does not interfere with VSV-GFP infection efficiency. Un-transfected H4 cells and H4 cells transiently transfected with WT aSyn and an empty vector control (pcDNA3.1) were cultured in high glucose DMEM supplemented with 10% FBS. Un-transfected H4 cells were treated with increasing concentrations of LPS. Cells were subsequently infected with VSV-GFP (MOI 0.5) for 24 hours. Fluorescent microscopy images of cells post-infection are displayed. LPS-treated cells displayed no reduction in GFP-signal compared to the un-transfected control (L2000). Scale bars, length 100 microM.

Testing possible anti-viral properties of mutant aSyn constructs via fluorescent microscopy.

One theory suggested by our lab to the large variability of observed within the transient transfection model in H4 cells was promotor competition. If so, we believed that the CMV promotor itself in the empty vector could be inhibiting viral replication (and thus GFP production), given that there was no gene-of-insert to be transcribed. To overcome the possibility of this promoter competition, I sought to incorporate another vector construct encoding a non-aSyn gene to aid as an experimental control. Gamma-synuclein (gSyn) is another member of the synuclein family; however, it is not as abundantly expressed within the brain and has not been thought to contribute to the formation of Lewy bodies in PD patients. While this construct was not intended to be used as a comparative control between different aSyn constructs and their respective experimental outcomes, it was intended to be used to control for experimental reliability/accuracy between replicated experimental runs. Ideally, the number of GFP-positive cells following VSV-GFP infection in gSyn transfected cells would be consistent between experimental replicates; however, this was not the case. Unfortunately, variability in the amount of observable GFP signal existed similarly to that of the empty vector controls used in the study. Still, the gSyn construct was incorporated into the results of this study when comparing the effects that different mutated forms of aSyn had on viral infections in cells.

As mentioned, the main goal of my thesis project was to determine how different mutations in aSyn could affect microbial infections within neurons. Previous studies within our lab examined the ability of different mutated forms of aSyn to alter viral infections within various models (i.e. H4 neuroglioma cells and *in vivo* models) (Rousso, 2019). During VSV-GFP infections, it was found that WT aSyn possessed protective qualities against infection, while mutations of aSyn (namely the disease-linked A53T and E46K mutant proteins) had a lesser

protective effect (Rousso, 2019). To further validate these findings and study additional mutations of aSyn, various constructs were cloned into different vector backbones (pcDNA3.1 or pDEST) and transiently transfected into H4 neuroglioma cells. A summary of the constructs studied can be seen in **Figure 2 and Table** 1. Two different vector backbones were used in part to test the reproducibility of the experimental model, as well as to incorporate additional mutant aSyn constructs that were gifted to our lab by Dr. Max Rousseaux. Of note, within the pDEST backboned vectors, some constructs contained a C-terminal 3x Flag tag while others lacked a flag. To ensure that the use of a 3x Flag tag did not affect the experimental outcomes, comparisons were made between different aSyn mutants in both the presence/absence of the 3x Flag (**Figure 6**). Fluorescent microscopy and quantification thereof did not indicate any statistically relevant differences, and data generated with/without a 3x Flag of the same aSyn genetic sequence was thereby complied in further experiments.

Continuing with the study of the present aim, H4 cells were transfected with 0.5µg of DNA encoding either gSyn, WT- or mutant aSyn. Each experimental run included empty vector controls of either pcDNA3.1 or pDEST vectors, as informed by which plasmid backbone the aSyn constructs being tested were closed into. Twenty-four hours post- transfection, cells were infected with VSV-GFP at 0.1 MOI and left for 20 hours as previously optimized. This MOI was chosen to allow for a long duration infection, with minimal cell death. To test my primary aim, being to quantify virus signal as a measure of infectivity, I first examined the level of GFP fluorescence via direct immunofluorescence (**Figure 7A & Figure 8A**). Prior to fluorescent imaging, cells were fixed with 4% PFA to avoid the cells lifting and to ensure a more accurate analysis. Fixation of cells was studied in optimization steps to confirm that GFP signal was affected. Following immunofluorescent imaging, quantification of the number of GFP-positive

cells was analyzed using ImageJ software (**Figure 7B & Figure 8B**). All results were normalized to the empty vector control within the respective vector backbone (i.e. pcDNA3.1 or pDEST). Neither immunofluorescence nor the quantification thereof identified any significant changes in the number of GFP-positive cells amongst the different aSyn mutations or WT aSyn as compared to their respective vector control. However, trends between replicate experiments would suggest that the number of GFP-positive cells is reduced in the presence of aSyn, with some mutated forms (i.e. A30P, A53T and E46K) having a lesser effect, and other mutations (i.e. G51D, S129A, d119 and 3xA-P) having an equal/greater effect than WT aSyn. The lack of statistical significance could be attributed to the large variability in the data between experimental replicates. To observe these findings in greater detail, indirect immunofluorescence was performed on select aSyn constructs of interest (**Figure 9**). Here, cells were fixed and stained for aSyn (Syn1), VSV and DAPI. Confocal microscopy analysis of the stained cells revealed similar results to that of the direct immunofluorescence analyses, where decreased total GFP-signal was visualized in cells transfected with S129A, d119 and G51D aSyn mutants compared to the vector control. This provides further evidence for the trends observed in the previous data set; however, the large variability between experimental replicates still limited the ability to draw definitive conclusions.

Flow cytometry methodology to revisit a biological effect by aSyn on VSV replication

To address this variability further, a more sensitive approach was utilized to evaluate how different mutations/variations of aSyn could affect microbial infections within neurons while still looking at GFP-signal as a primary readout. Flow cytometry analysis was performed, again comparing the total number of GFP-positive cells in infected cells to that of mock-treated cells (**Figure 10A/B & Figure 11A/B**). To control for cell death as another possible contributing factor

relating to experimental variability, cells were stained with a viability dye (Zombie NIR) prior to fixation and analysis. This was done to evaluate whether cell death was increased/decreased between experimental replicates, and also between mock and infected cells. When examining whether different aSyn constructs altered the number of GFP-positive cells, no significant differences were observed. In addition, GFP signal intensity was evaluated and again showed no statistically significant differences between any aSyn construct compared to the respective vector control (**Figure 10B & Figure 11B**). Interestingly, WT aSyn (pcDNA3.1) produced a trend of increased GFP-positive cells compared to the vector control. This trend was not observed within the pDEST vector backbone. Although statistically insignificant, this trend is in contrast to the findings conducted by fluorescent microscopy. Other mutant forms of aSyn within both vector backbones seemed to follow similar trends as observed in previous fluorescent microscopy analysis. Similarly to that of the fluorescent microscopy analysis, within the pDEST vector backbone, the G51D, S129A, d119 and 3xA-P mutations each seemed to behave similarly to WT aSyn in the context of decreasing the total number of GFP-positive cells following infection. As well, both A53T and A30P mutations seemed to have a lesser effect than WT aSyn at minimizing viral spread. However, while observing the higher number of GFP-positive cells of the WT aSyn containing a pcDNA3.1 vector backbone, the accompanying mutations (A53T and E46K) appeared to have a greater effect at minimizing GFP-positive cells. A summary of these observations can be found in **Table 2.** While certain trends do seem to exist, they lack significance. Again, this could be attributed to large variability between experimental replicates, which was unfortunately not overcome using the more sensitive Flow cytometry approach.

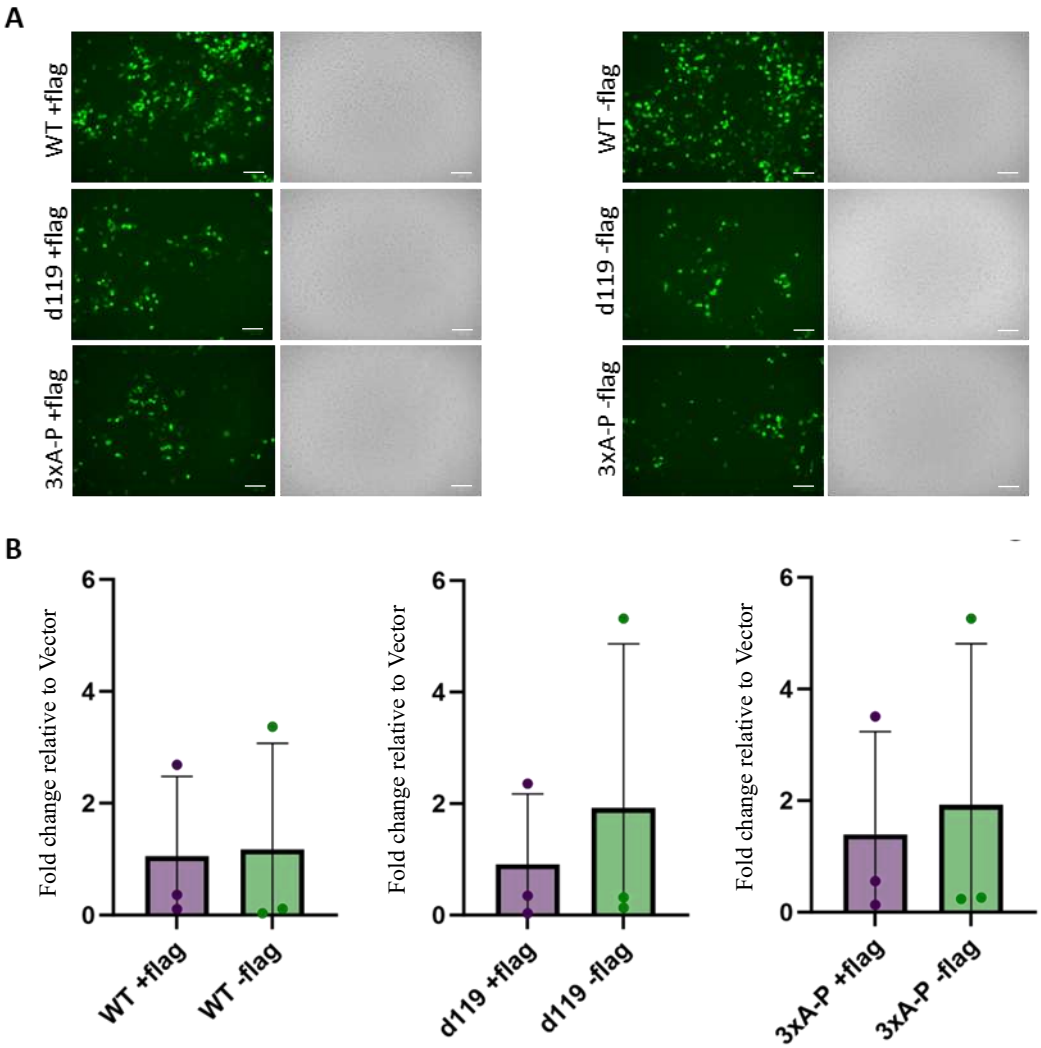

Fig 6. The presence/absence of a triple flag in the aSyn protein sequence generated comparable results in different experimental readouts. H4 cells transiently transfected to express either WT or mutated aSyn with/without an attached 3xflag tag were cultured in high glucose DMEM supplemented with 10% FBS and subsequently infected with VSV-GFP (MOI 0.1) for 20 hours. **(A)** Fluorescent microscopy images (GFP, DAPI, bright-field) were captured to confirm no differences in viral replication/GFP production between similar aSyn formations with/without a 3xflag tag. Scale bars, length 100 microM. **(B)** Quantification of total fluorescent GFP signal was performed using ImageJ. No significant differences were observed by student T-test ($P>0.05$).

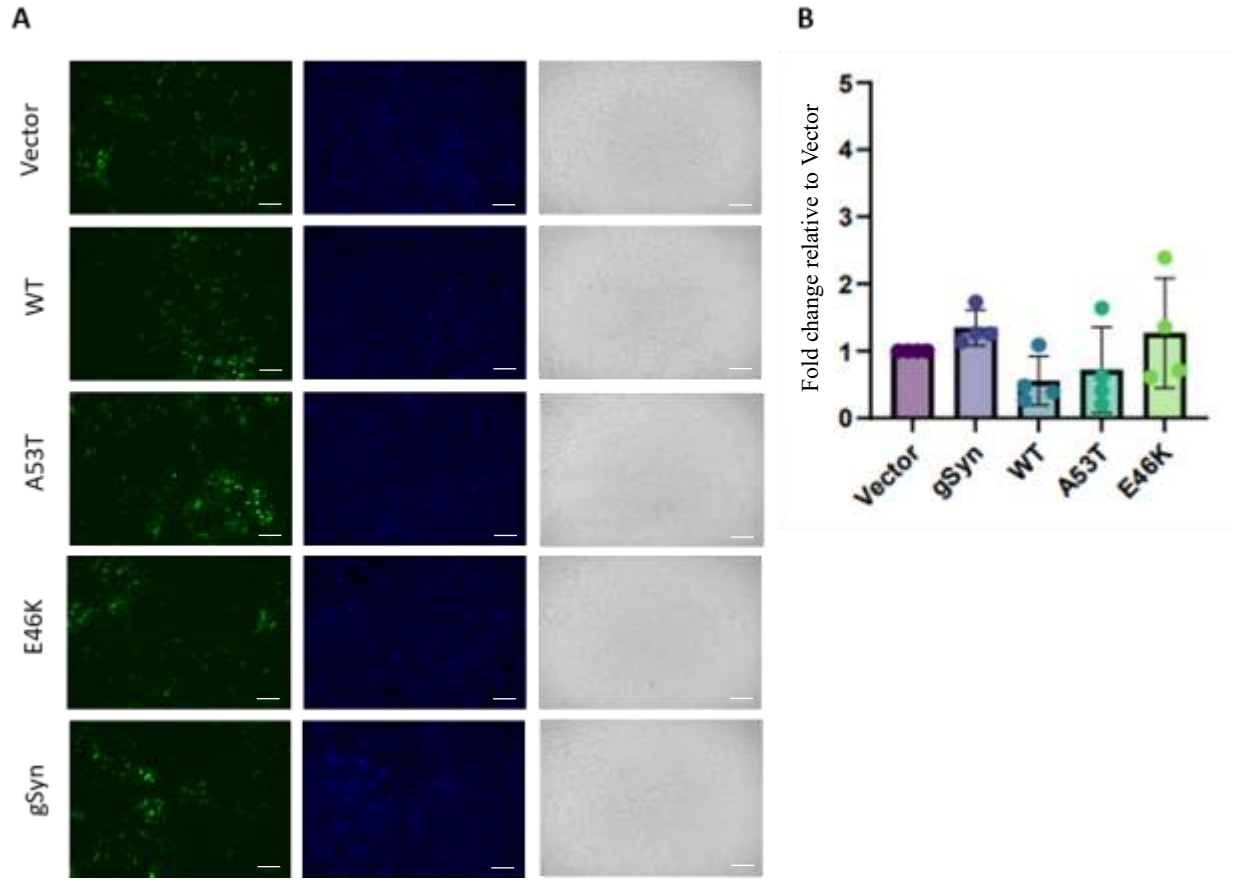

Fig 7. pcDNA3.1 aSyn constructs do not confer protective qualities against VSV-GFP infection in H4 cells compared to the vector control via fluorescent microscopy. H4 cells transiently transfected to express either WT or mutant aSyn were cultured in high glucose DMEM supplemented with 10% FBS and subsequently infected with VSV-GFP (MOI 0.1) for 20 hours. **(A)** Fluorescent microscopy images (GFP, DAPI, bright-field) were captured to assess viral replication. Scale bars, length 100 microM. **(B)** Quantification of total fluorescent GFP signal was performed using ImageJ. No significant differences were observed by one-way ANOVA test ($P>0.05$).

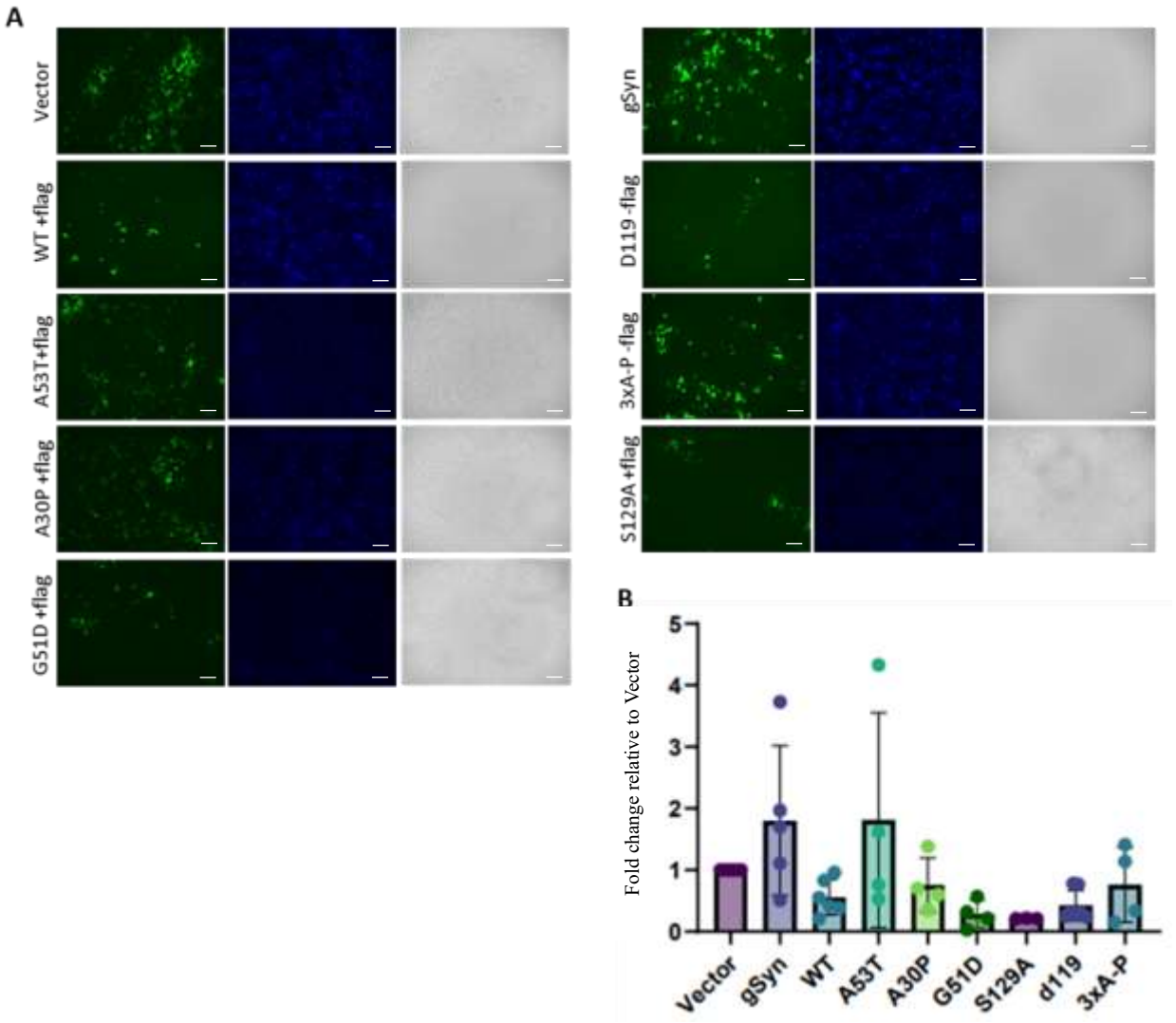

Fig 8. Fluorescent microscopy does not reveal protective qualities of aSyn in all tested aSyn constructs with a pDEST vector backbone compared to the vector control. H4 cells transiently transfected to express either WT or mutant aSyn were cultured in high glucose DMEM supplemented with 10% FBS and subsequently infected with VSV-GFP (MOI 0.1) for 20 hours. **(A)** H4 cells transiently transfected to express either WT or mutated aSyn were cultured in high glucose DMEM supplemented with 10% FBS and subsequently infected with VSV-GFP (MOI 0.1) for 20 hours. Fluorescent microscopy images (GFP, DAPI, bright-field) were captured to assess viral replication. Scale bars, length 100 microM. **(B)** Quantification of total fluorescent GFP signal was performed using ImageJ. No significant differences were observed by one-way ANOVA test ($P>0.05$).

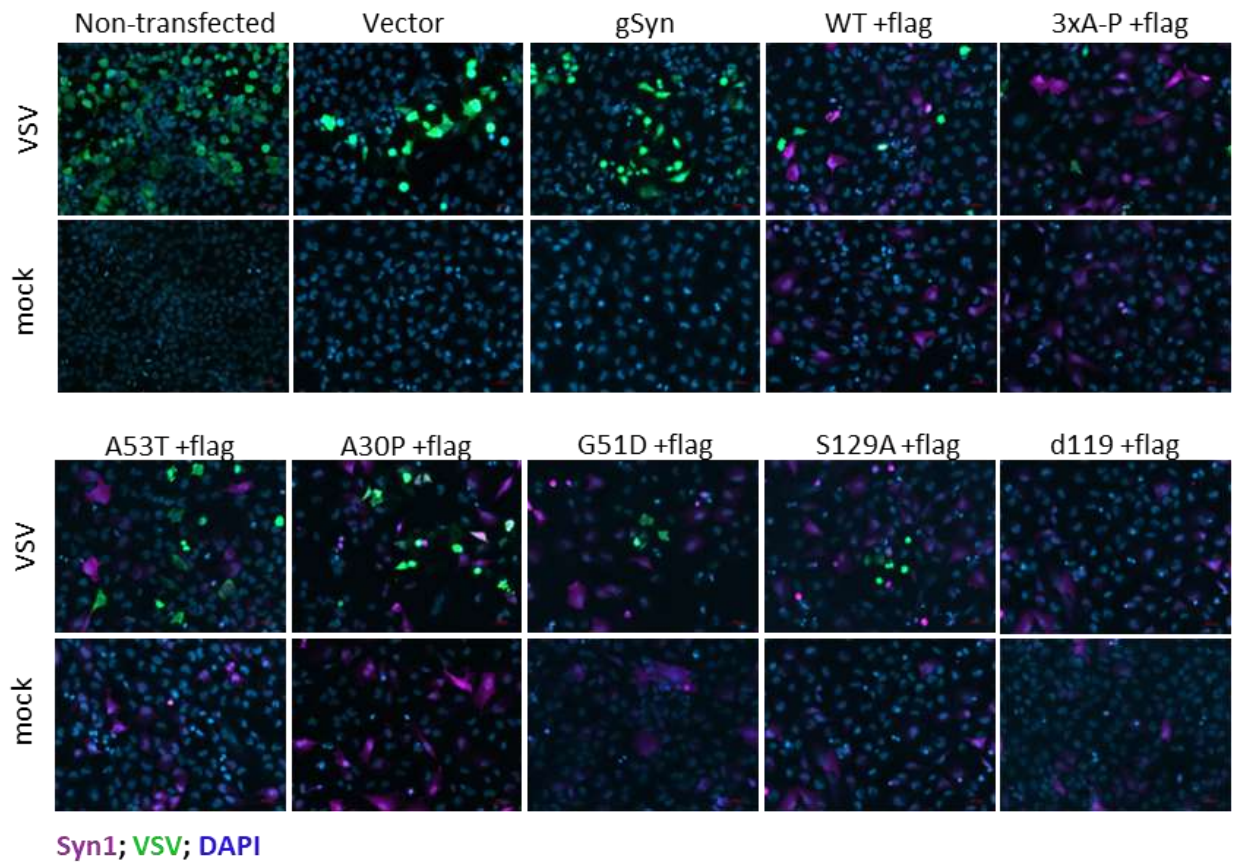

Fig 9. Indirect immunofluorescence staining demonstrates trends in decreased VSV-GFP infectivity in mutated aSyn expressing H4 cells. H4 cells transiently transfected to express either WT or mutant aSyn were cultured on cover slips in high glucose DMEM supplemented with 10% FBS and subsequently infected with VSV-GFP (MOI 0.1) for 20 hours. Indirect immunofluorescent staining was performed to stain for aSyn (purple), VSV-GFP (green) and DAPI (blue). Images were taken at 40x magnification. Scale bars, length 100 microM.

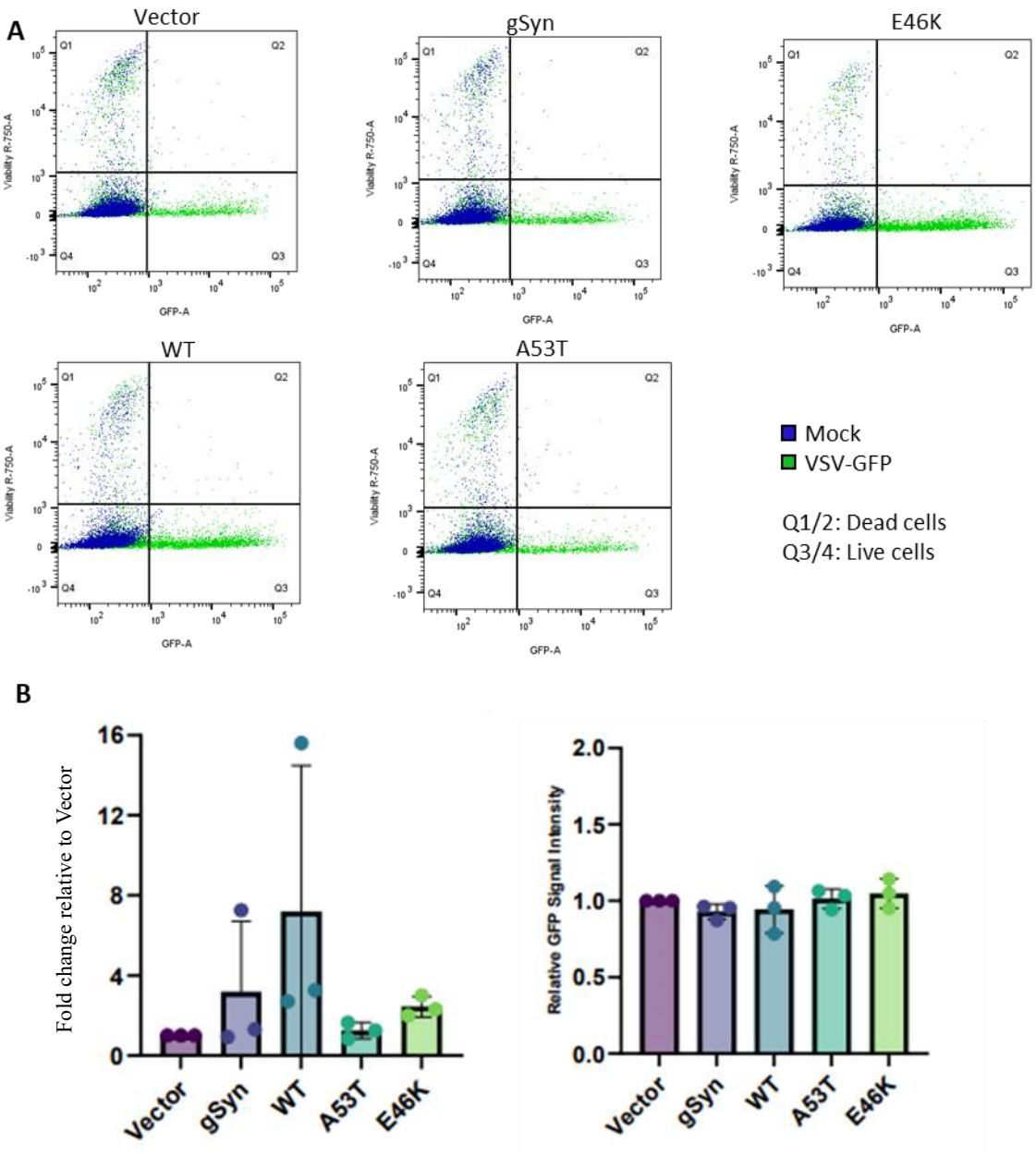

Fig 10. Flow cytometry does not reveal protective qualities of aSyn in all tested aSyn constructs containing a pcDNA3.1 vector backbone compared to the vector control. H4 cells transiently transfected to express either WT or mutant aSyn were cultured in high glucose DMEM supplemented with 10% FBS and subsequently infected with VSV-GFP (MOI 0.1) for 20 hours. **(A)** H4 cells transiently transfected to express either WT or mutated aSyn were cultured in high glucose DMEM supplemented with 10% FBS and subsequently infected with VSV-GFP (MOI 0.1) for 20 hours. Cells were harvested and stained with Zombie NIR for cell viability to be used in flow cytometry analysis. **(B)** Quantification of total fluorescent GFP signal and GFP signal intensity was performed using ImageJ. No significant differences were observed by one-way ANOVA (P>0/05).

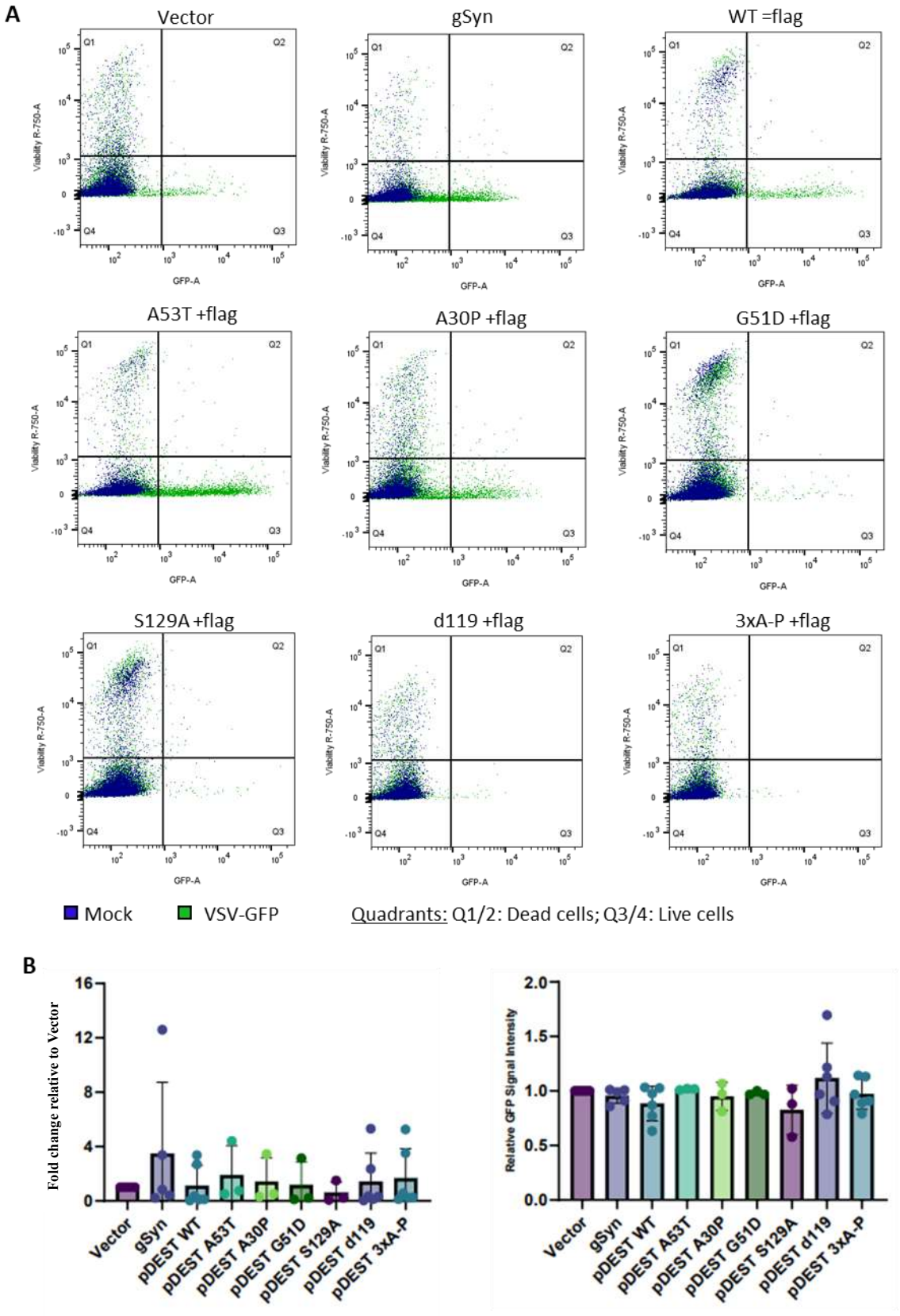

Fig 11. No alterations in GFP-signal following VSV-GFP infection in H4 cells expressing various conformations

of aSyn with a pDEST backbone are observe compared to the vector control. H4 cells transiently transfected to express either WT or mutant aSyn were cultured in high glucose DMEM supplemented with 10% FBS and subsequently infected with VSV-GFP (MOI 0.1) for 20 hours. **(A)** H4 cells transiently transfected to express either WT or mutated aSyn were cultured in high glucose DMEM supplemented with 10% FBS and subsequently infected with VSV-GFP (MOI 0.1) for 20 hours. Cells were harvested and stained with Zombie NIR for cell viability to be used in flow cytometry analysis (outsourced). **(B)** Quantification of total fluorescent GFP signal and GFP signal intensity was performed using ImageJ. No significant differences were observed by one-way ANOVA test ($P>0.05$).

Table 2. Summary of the comparisons between WT aSyn and respective aSyn mutations following VSV-GFP infections via fluorescent readouts.

aSyn Mutation	Fluorescent Microscopy	Flow Cytometry
A53T	Increased GFP expression compared to WT	Increased GFP expression compared to WT (pDEST) Decreased GFP expression compared to WT (pcDNA3.1)
A30P	Increased GFP expression compared to WT	Increased GFP expression compared to WT
E46K	Increased GFP expression compared to WT	Increased GFP expression compared to WT
G51D	Decreased GFP expression compared to WT	Decreased/equivalent GFP expression compared to WT
S129A	Decreased/equivalent GFP expression compared to WT	Decreased/equivalent GFP expression compared to WT
d119	Decreased/equivalent GFP expression compared to WT	Equivalent GFP expression compared to WT
3xA-P	Decreased/equivalent GFP expression compared to WT	Equivalent GFP expression compared to WT

In addition to fluorescent analyses, Western blot analyses of lysates of mock versus infected cells were conducted to visualize and quantify VSV protein expression (**Figure 12A & Figure 13A**). Similar to the findings from fluorescence and FACs-based analysis, cells that were transfected with different aSyn constructs did not reveal any significant differences in VSV protein expression (**Figure 12B**) compared to the vector control; however, there appeared to be an indication that the E46K aSyn mutation yields higher expression of VSV proteins compared to WT and A53T-mutated aSyn. The elevated expression of VSV proteins may be indicative of higher VSV gene copy numbers, and thus increased infection. Similarly to the E46K mutation, there did seem to be a trend in the quantified data suggesting higher increases in VSV protein expression in both the A53T and A30P aSyn mutations (**Figure 13B**). This trend reflects the results observed through immunofluorescence analysis which indicated that the two mutations follow a pattern of increased GFP-signal, and thus possibly increased viral infection rates. In the same instance, the G51D mutation appeared to continuously reveal decreased VSV protein expression, which again matches the trends observed within the previous immunofluorescence studies, which were indicative of decreased GFP-signal. While these trends were present, no statistically significant quantitative conclusions could be drawn. The lack of significance could, again, be attributed to the large variability, specifically within the vector control-transfected cells. This variability can be easily observed between the two separate blots in **Figure 13A**, where each blot contains an independent pDEST vector control sample. The vector control in the first blot shows high VSV protein expression compared to the near lack of expression that can be observed in the second.

Investigating the consequences of different aSyn mutations following VSV-GFP infection

While the primary aim of this study was to determine if different aSyn mutations were able to impact viral infections, the secondary aim was then to test if viral infections could initiate changes in aSyn expression/metabolism itself. To address this second aim, parallel studies were conducted through Western blot analysis to detect changes in aSyn expression and possible post-translational modifications at the protein level (via Syn1 antibody) (**Figure 12A & Figure 13A**). Through quantification of the aSyn protein levels on the Western blot, cells that were transfected with the various aSyn constructs mostly did not reveal statistically significant differences in aSyn protein expression following VSV-GFP infection compared to mock treated cells (**Figure 12C & Figure 13C**). Yet, by qualitatively looking at the blots themselves and the accompanying quantification analysis, a small but statistically insignificant decrease in aSyn protein expression within each tested construct could be observed following infection. Of note, a statistically significant increase in 3xA-P aSyn protein expression compared to the vector control was observed; however, this expression did not change between mock and infected samples within the mutant itself. (**Figure 13C**). Thus, the significance does not reveal any information relative to whether VSV-GFP infections contributed to altered protein expression within this specific mutation. Additionally, no higher molecular weight species been indicative of oligomeric / multimeric forms of aSyn were observed on the blots. It should also be noted that while large variability was still observed within the vector control arms, variability was evident among the aSyn expressing constructs as well.

Overall, the analyses conducted by transiently transfecting various aSyn-encoding constructs into human neuronal (H4) cells did not reveal any significant differences in the level of VSV-GFP infection as observed through GFP-signal quantifications, nor in aSyn protein

expression following said infections. Still, some trends in the data can be observed that may suggest decreased infection (via decreased GFP-signal production) and thus a potentially protective effect of aSyn against VSV-GFP infection. That being said, the reliability of these observations can be questioned given the variability between experiments in all readouts performed. Of note, the gSyn construct incorporated also produced variable results in each experimental readout. This concludes that the theory of CMV-promotor competition does not bear much merit, and the issues of inconsistency must be attributed to something else. As such, another cell model was introduced to test similar aims in later experiments.

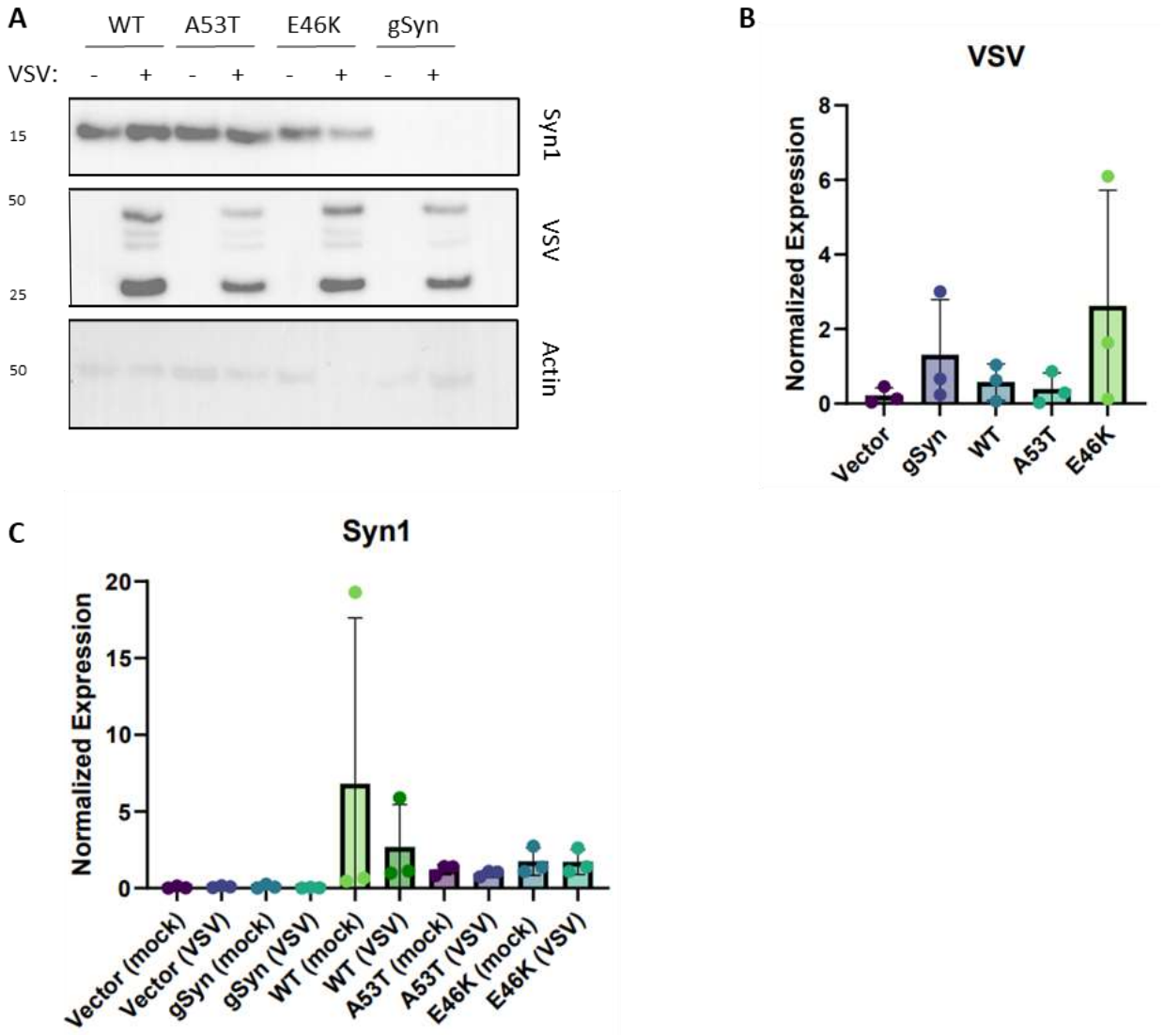

Fig 12. Protein expression of VSV and aSyn are not significantly altered post VSV-GFP infection in H4 cells expressing pcDNA3.1 aSyn constructs compared to the vector control. (A) H4 cells transiently transfected to express either WT or mutated aSyn were cultured in high glucose DMEM supplemented with 10% FBS and subsequently infected with VSV-GFP (MOI 0.1) for 20 hours. Cells were harvested and lysed in Triton X-100 buffer. Lysates were run on a 4-12% Bis-Tris gel for Western blot analysis against aSyn and VSV, and beta-actin. **(B,C)** Quantification of VSV and aSyn (Syn1) total expression was calculated using ImageJ and normalized to beta-actin. No significant differences were observed by one-way ANOVA test ($P>0.05$).

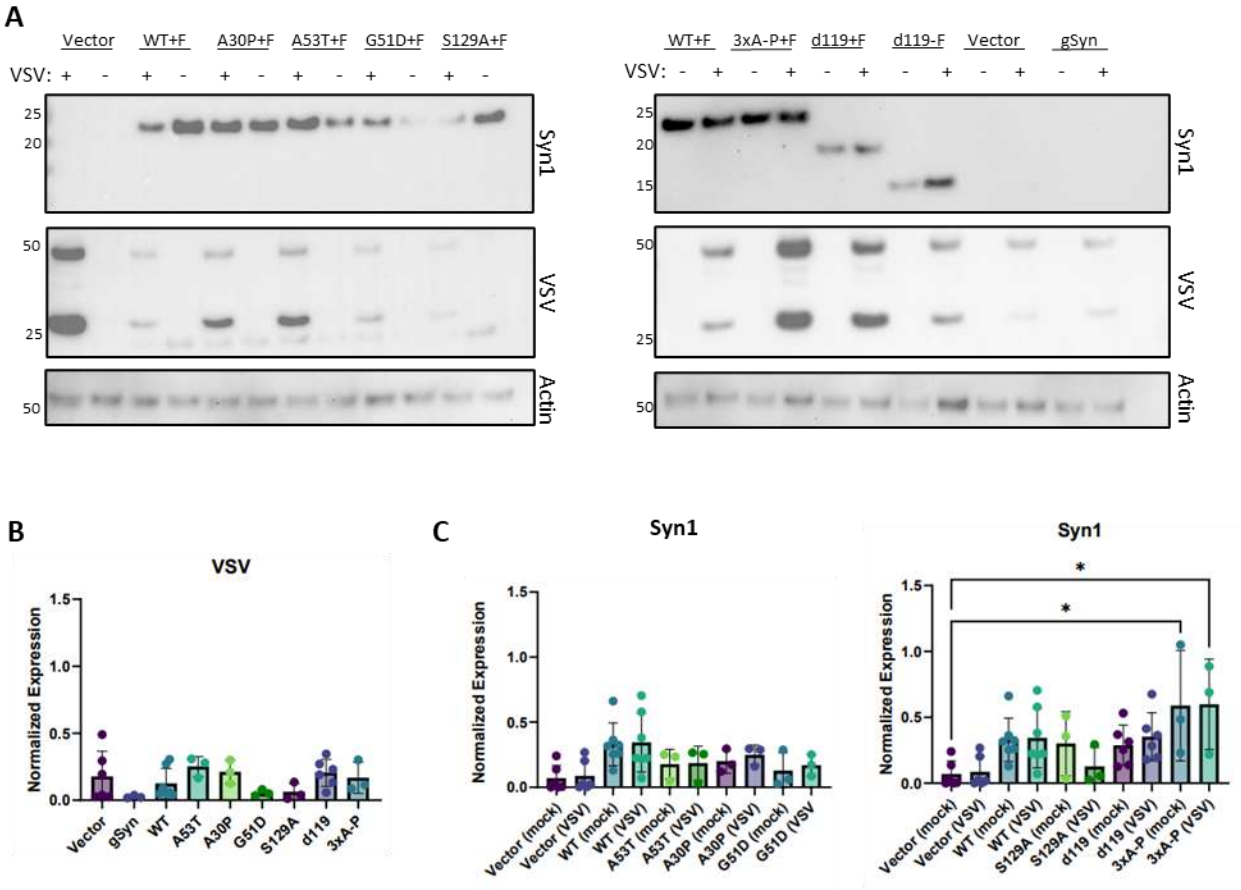

Fig 13. VSV and aSyn protein levels are not significantly altered post VSV-GFP infection in H4 cells expressing pDEST aSyn constructs compared to the vector control. (A) H4 cells transiently transfected to express either WT or mutated aSyn were cultured in high glucose DMEM supplemented with 10% FBS and subsequently infected with VSV-GFP (MOI 0.1) for 20 hours. Cells were harvested and lysed in Triton X-100 buffer. Lysates were run on a 4-12% Bis-Tris gel for Western blot analysis against aSyn and VSV, and beta-actin. **(B,C)** Quantification of VSV and aSyn (Syn1) total expression was calculated using ImageJ and normalized to ponceau stain. No significant differences were observed by one-way ANOVA test ($P>0.05$).

Alterations in viral infection are not observed following VSV-GFP infection of non-human catecholamine producing cells in an aSyn Tet-off model

Due to the possibility of transient transfections leading to variability in the previous approach, I tested my hypothesis in a second, previously established, doxycycline-controlled aSyn over-expression cell model. These PC12-C4 cells stably overexpress human *SNCA* under normal conditions (PC12-C4 -dox); however, *SNCA* gene over-expression can be silenced with the addition of doxycycline (PC12-C4 +dox). Of note, parental, non-human *SNCA*-expressing PC12 cells were used in the presence/absence of doxycycline as an experimental control. This model is ideal for testing the ability of WT aSyn to alter VSV-GFP infections as it minimizes the need for transient transfections, which was a potential source of variability observed in the H4 cell-based model. This model, however, is only established using WT aSyn. Prior to addressing the aims of this study, optimization of the amount of doxycycline needed to effectively silence *SNCA* expression was performed. Increasing concentrations of doxycycline were added to PC12-C4 cells and after 5 days of treatment, the cells were harvested and lysed for Western blot analysis to probe for aSyn signals (using the antibody Syn1) (**Figure 14A**). Results showed that 200ng/ml of doxycycline was sufficient to silence *SNCA* expression down to endogenous levels and was thus the concentration chosen to use throughout the remaining study.

The primary aim using this model was to test whether WT human aSyn could confer protective effects against viral infections. To address this, VSV-GFP was utilized as above. These cells were more sensitive to infection, which led to more cell death at the same MOI of infection compared to H4 cells, and thus adjustments in the conditions used for infection were made: an MOI of 3.0 VSV-GFP was used to infect the cells for a total duration of three hours. As done

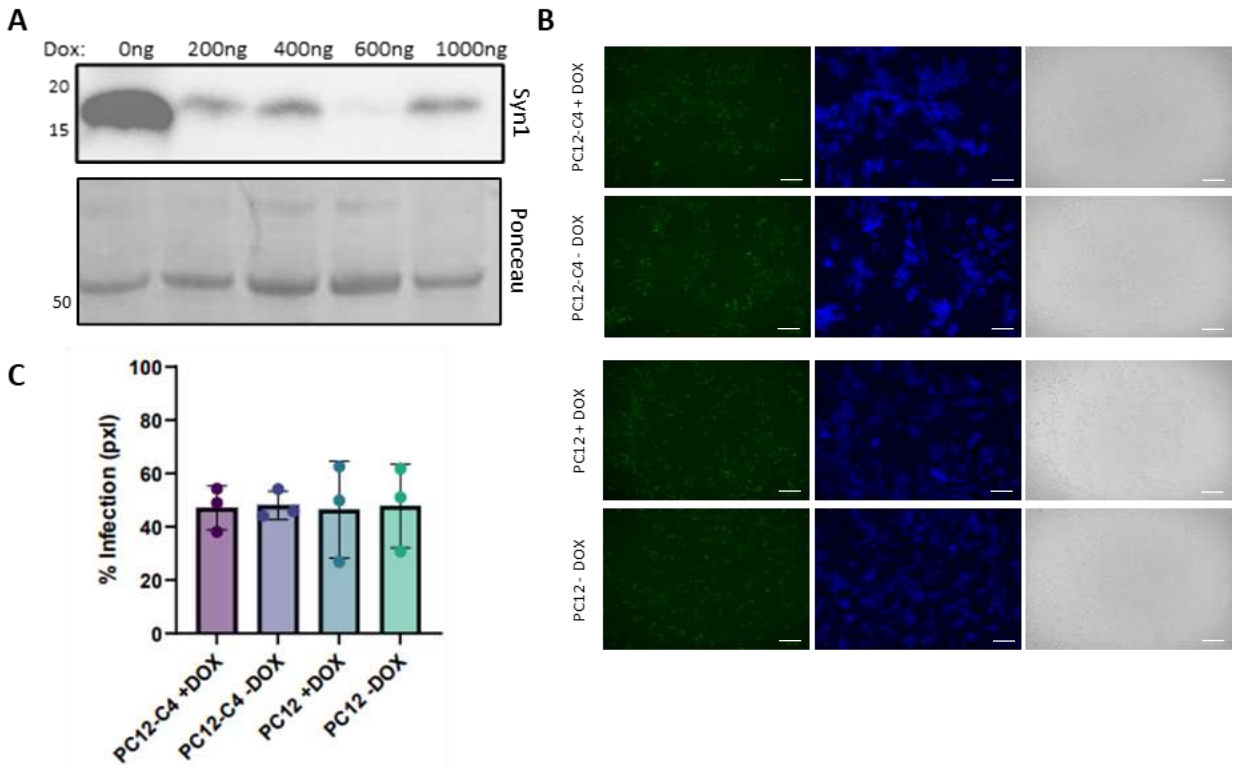

Fig 14. Fluorescent microscopy analyses indicate the overexpression of aSyn does not alter VSV-GFP infections. **(A)** Untransfected PC12 cells and PC12 cells stably transfected with human *SNCA* (PC12-C4) were treated with increasing concentrations of doxycycline (DOX) for optimization. Cells were harvested and lysed in Triton X-100 buffer. Lysates were run on a 4-12% Bis-Tris gel for Western blot analysis against aSyn. **(B)** Untransfected PC12 cells and PC12 cells stably transfected with human *SNCA* (PC12-C4) were cultured in DMEM with/without 200ng/ml DOX (dox) and infected with VSV-GFP (MOI 3) for 3 hours. Fluorescent microscopy images (GFP, DAPI, bright-field) captured to assess viral replication in PC12-C4 and PC12 cells +/-DOX. Scale bars, length 100 microM. **(C)** Quantification of total fluorescent GFP signal was performed using ImageJ. No significant differences were observed by one-way ANOVA test ($P>0.05$).

previously, direct immunofluorescence was conducted to monitor the GFP signal in each cell condition tested (i.e. PC12-C4 +dox, PC12-C4 -dox, PC12 +dox, PC12 -dox) (**Figure 14B/C**). Both the immunofluorescent images captured, and the quantification thereof, revealed no statistically significant difference in GFP-positive cells between each tested condition. I concluded that the silencing of human WT aSyn over-expression did not alter the rate of VSV-GFP infection and viral protein expression, and thus revealed no protective qualities of WT aSyn. Of note, the parental cells (PC12) demonstrated no difference in GFP-signal in either the presence/absence of doxycycline.

To confirm these findings using a more sensitive approach, flow cytometry was completed in parallel experiments (**Figure 15A**). As in previous studies, both the number of GFP-positive cells and the intensity of the GFP signal were quantified and normalized to mock treated cells (**Figure 15B/C**). No significant differences were observed between each tested condition, complementing the results obtained from the fluorescent microscopy-based analyses. As done in previous flow cytometry analyses, cells were stained with a viability dye (Zombie NIR) prior to fixation and analysis to evaluate whether cell death was increased/decreased between experimental replicates, and also between mock and infected cells. Overall, the results from each fluorescent microscopy and flow cytometry experiment indicated no protective qualities of WT aSyn against VSV-GFP infection.

After immunofluorescent and flow cytometry analysis was completed, Western blots against VSV were performed to confirm the initial findings at the protein level. Both qualitative and quantitative data revealed no changes in VSV protein expression when *SNCA* was silenced, revealing that the presence/absence of WT aSyn does not alter VSV-GFP infection in PC12-C4

cells (**Figure 16A/B**). Overall, I concluded that WT aSyn does not contain protective qualities against viral infections within this experimental model.

VSV-GFP infection does not elicit changes in aSyn protein expression of non-human catecholamine producing cells in an aSyn Tet-off model

Next, I aimed to address whether VSV-GFP infections could induce changes in the protein expression of WT aSyn. Western blots against aSyn using the Syn1 antibody were completed to address this question. Qualitative observations of the blot itself did not show changes between mock and infected cells within each tested condition (**Figure 16A**). This observation was confirmed through quantitative analysis (**Figure 16C**). As detailed, there was no significant increase/decrease in WT aSyn protein level itself following VSV-GFP infection compared to mock treated cells, providing evidence that WT aSyn steady-state was not altered in response to infection. Additionally, higher molecular weight species were not observed, similar to the findings in the previous cell model. Overall, VSV-GFP infections did not confer an altered state of WT aSyn in the current cell model.

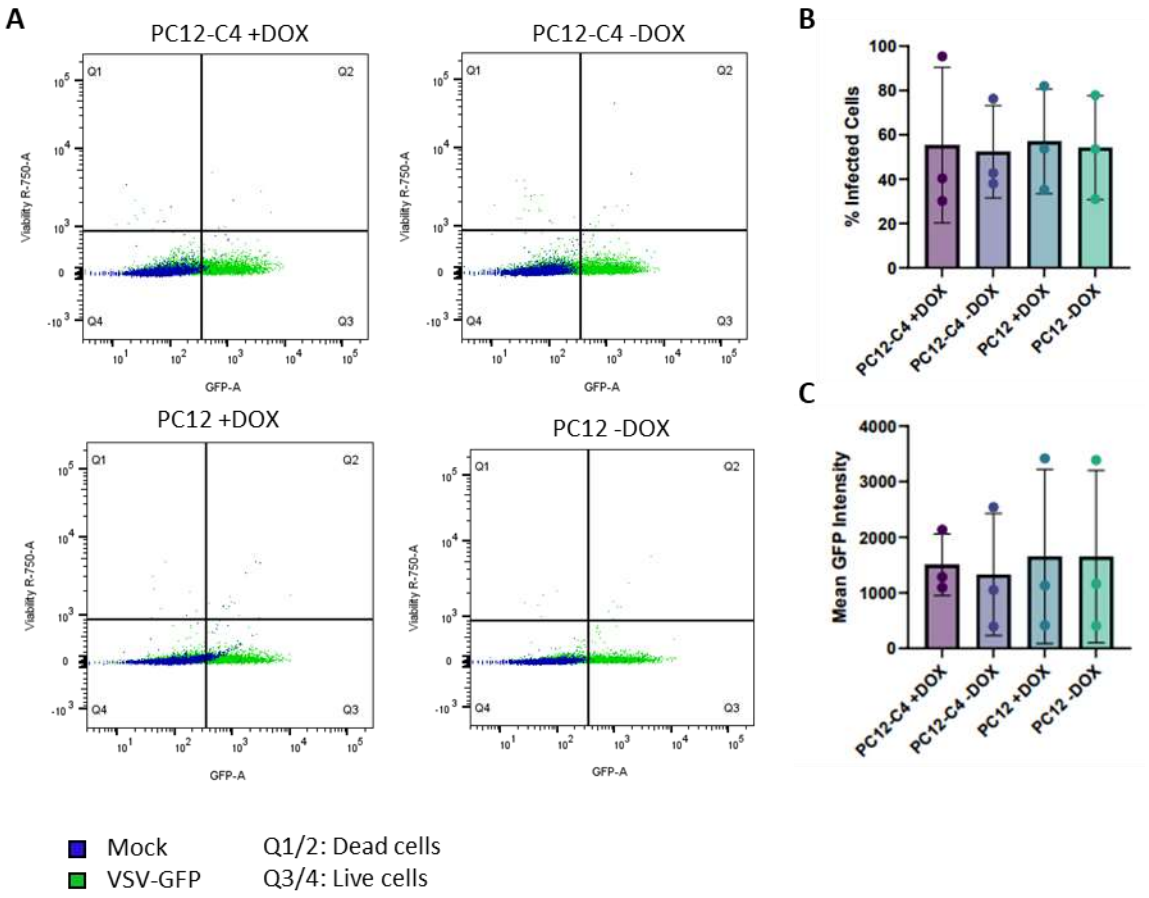

Fig 15. The overexpression of aSyn does not produce alterations in GFP-signal following VSV-GFP infection in PC12-C4 cells via flow cytometry. The overexpression of aSyn does not alter VSV-GFP infections via flow cytometry. (A) Untransfected PC12 cells and PC12 cells stably transfected with human *SNCA* (PC12-C4) were cultured in DMEM with/without 200ng/ml DOX (dox) and infected with VSV-GFP (MOI 3) for 3 hours. Cells were harvested and stained with Zombie NIR for cell viability to be used in flow cytometry analysis. **(B,C)** Quantification of total fluorescent GFP signal and GFP signal intensity was performed using ImageJ. No significant differences were observed by one-way ANOVA test (P>0.05).

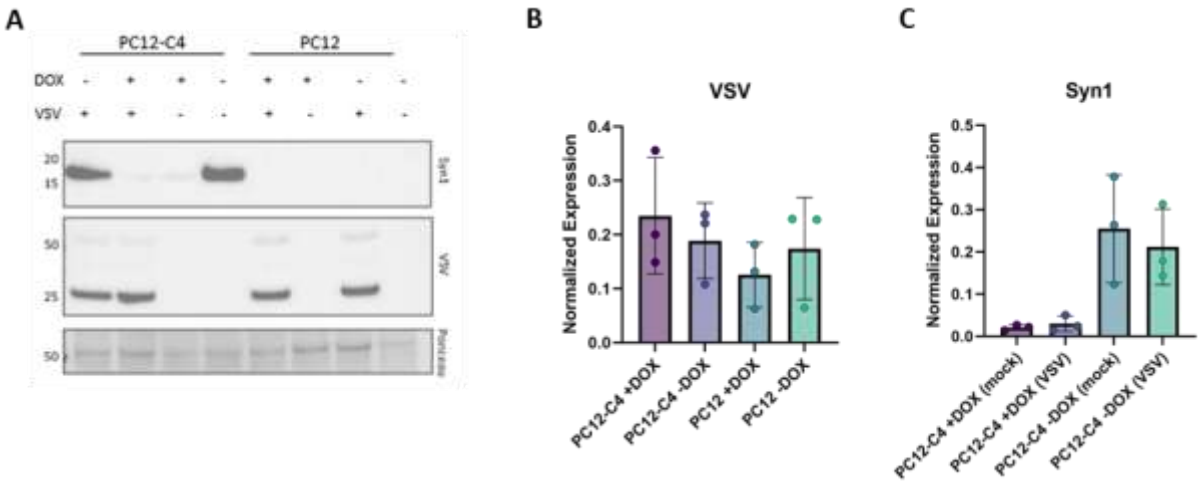

Fig. 16. Western blot analyses do not reveal differences in VSV or aSyn protein expression following VSV-GFP infection in PC12-C4 cells. (A) PC12-C4 cells were grown in DMEM with/without 200ng/ml DOX (dox) and infected with VSV-GFP (MOI 3) for 3 hours. Cells were harvested and lysed in Triton X-100 buffer. Lysates were run on a 4-12% Bis-Tris gel for Western blot analysis against aSyn, VSV, and beta-actin. **(B,C)** Quantification of VSV and aSyn (Syn1) total expression was calculated using ImageJ and normalized to ponceau stain. No significant differences were observed by one-way ANOVA test ($P>0.05$).

Aggregation of aSyn is increased following viral infection with VSV in human neuronal cells

The previous results revealed no alterations in the level of total aSyn protein expression produced following viral infection, nor did they reveal any changes/modification in protein conformation. Thus, to further examine what happens to the protein itself following viral infections, an aSyn oligomer-facilitating construct (BiSyn) was utilized. This construct encodes two copies of the human *SNCA* cDNA in a bi-cistronic plasmid design. One *SNCA* cDNA contains half of the GFP sequence located at its N-terminal, while the second *SNCA* cDNA contains the remaining GFP sequence at its C-terminal. In theory, if the two produced proteins were to combine to form an oligomer, the GFP sequence halves would fuse together and fluoresce, indicating the formation of a dimer (and possibly higher order multimers).

To address the experimental aim stated above, H4 cells were transiently transfected with the BiSyn construct and 24 hours later, they were infected with wild-type VSV (no GFP tag) for 24 hours at an MOI of 0.5. The MOI used for experimentation was previously optimized to cause the greatest level of infection with minimal cell death. Indirect immunofluorescent staining was performed post-infection for the detection of VSV (**Figure 17A**). Of note, GFP detection was observed through autofluorescence of the GFP proteins produced during experimentation. Quantification of GFP-positive cells showed a significant increase ($P<0.0001$) in aSyn oligomerization following VSV infection compared to mock-treated cells (**Figure 17B**) as attributed to the number of GFP-positive cells. Importantly, aSyn oligomerization did exist in the absence of VSV infections, but to a lesser extent. Of note, the *intensity* of the GFP signal produced within the mock treated and VSV infected cells did not significantly differ, yet, there is a clear increase in the *overall* production of GFP-signal when the cells were infected with VSV (**Figure 17C**)

To further validate these findings, Western blotting against both aSyn and VSV were performed (**Figure 17D-F**). Quantification analysis revealed that there was no significant increase in aSyn total expression, indicating that the amount of protein produced in the presence/absence of VSV did not change. Of note, no higher molecular weight species of aSyn (indicative of oligomerization) were detected on the Western blots. Taken together, the results conveyed that while the total level of aSyn produced did not change during viral infection, aSyn undergoes modifications contributing to the formation of detectable aggregates.

To further investigate the process of aSyn aggregation during microbial infection and the kinetics of an aSyn oligomerization event, time-lapse recordings of live-cell imaging following VSV infections were conducted. H4 cells transiently transfected to express BiSyn were infected at higher MOIs of VSV (MOI 3.0 and MOI 5.0) to cause rapid infection. Time-lapse recordings were captured across 20 hours in 15-minute intervals. These recordings were compared to mock-infected cells that were cultured in parallel. For the purpose of this report, still images from the same time-points are displayed (**Figure 18**). The results indicated that aSyn aggregation, although present in mock-infected cells, is increased when the cells are exposed to the viral pathogen as early as 5 hours post-infection. By the end of the infection period, it is evident that infected cells contained greater amounts of aSyn di-/oligomers than mock-infected cells. While the results gathered using the BiSyn construct require further assessment, such as of cell health, they suggested that aSyn undergoes modifications in the presence of microbial infection, which likely contributes to the higher molecular weight formation of the protein. Whether these are bona fide aggregates en route to Lewy inclusion-type formation, as seen in PD brains, remains to be tested.

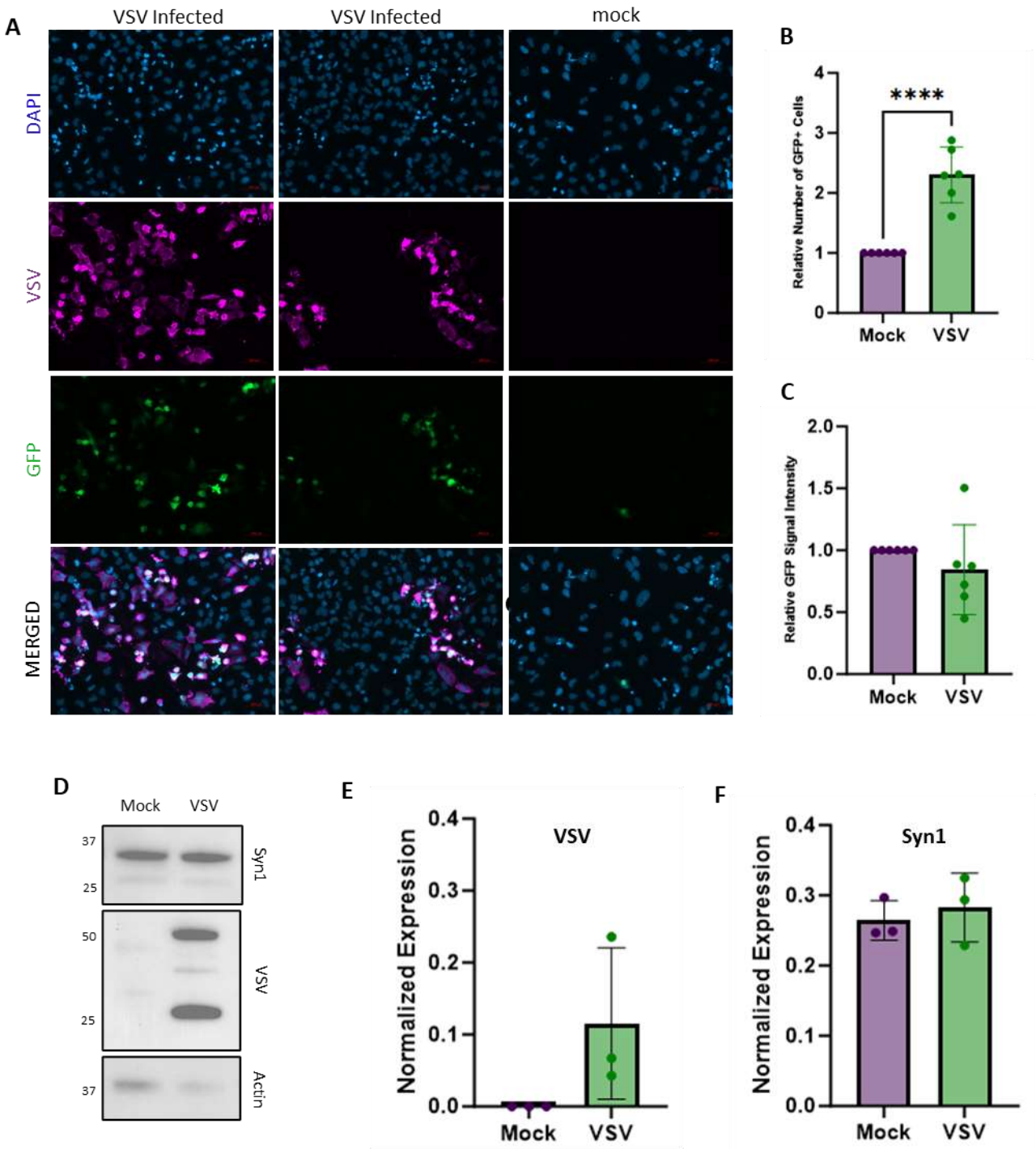

Fig 17. VSV infection promotes aSyn oligomerization. (A) Indirect immunofluorescent staining was performed to stain for VSV (purple) and DAPI (blue). Images were taken at 40x magnification. Scale bars, length 100 microM. **(B,C)** Statistically significant differences were observed between total GFP signal (aSyn aggregates) in infected cells normalized to mock cells ($P<0.0001$). No significant difference was observed between GFP signal intensity in infected cells normalized to mock cells ($P>0.05$). **(D)** Cells were harvested and lysed in Triton X-100 buffer. Lysates were run on a 4-12% Bis-Tris gel for Western blot analysis against aSyn and VSV, and beta-actin. **(E,F)** Quantification of VSV and aSyn (Syn1) total expression was calculated using ImageJ and normalized to ponceau stain. No significant differences in aSyn expression were observed by one-way ANOVA test ($P>0.05$).

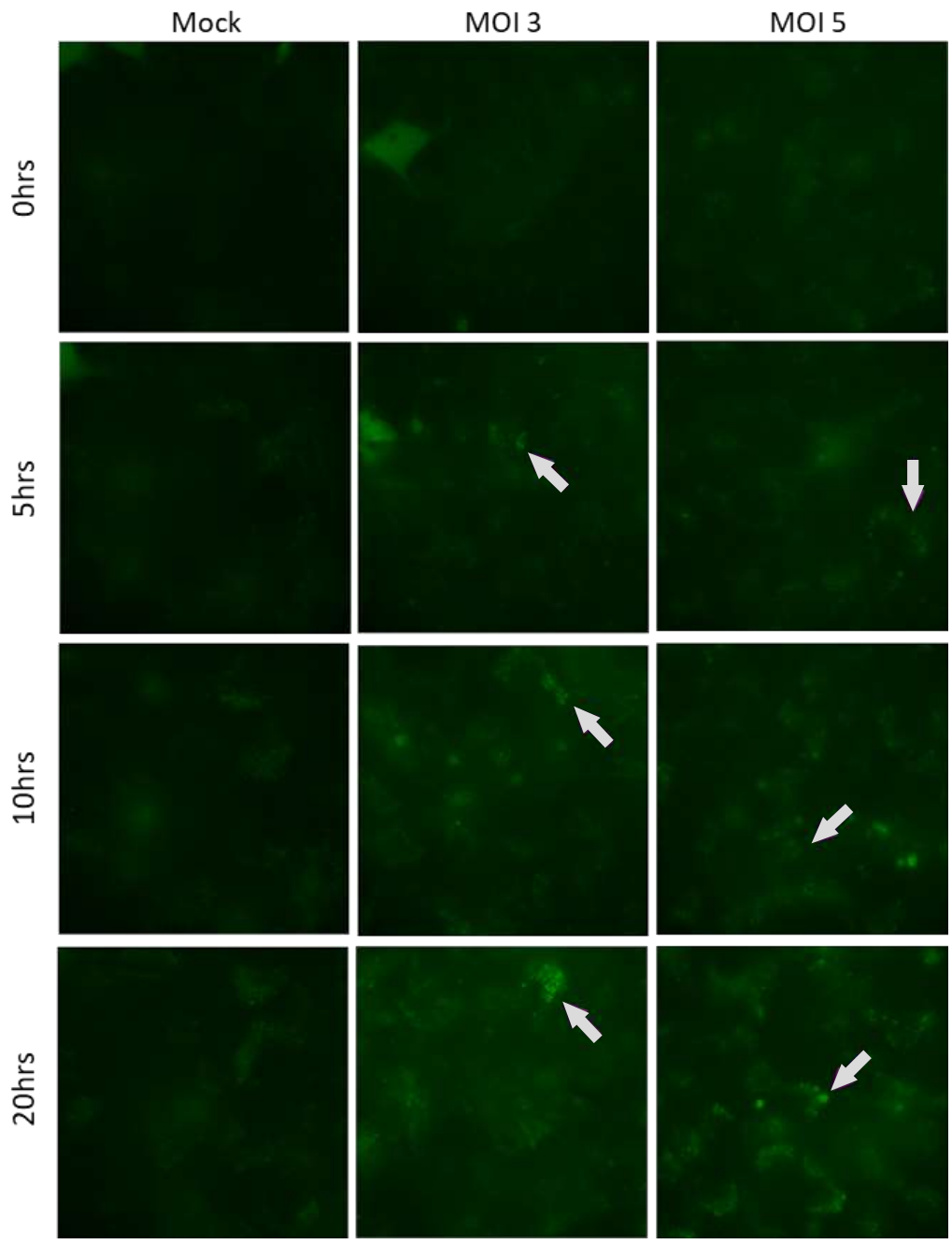

Fig 18. Time-Lapse analysis of aSyn aggregation accumulation in H4 neuronal cells. H4 cells transiently transfected to express a BiSyn construct were cultured in high glucose DMEM supplemented with 10% FBS and subsequently infected with increasing MOIs of VSV for 20 hours. Live-cell images were captured every 15 minutes for the duration of infection and compiled to form a time-lapse video. Still images were taken from each video at specific time-points to show increasing aSyn aggregates (examples notated via arrows).

Chapter 4. Discussion

The hypothesis that microbial infections could be an environmental trigger of PD has led to the study of aSyn and its biological functions outside of the brain. Uncovering whether aSyn plays an active role in the innate immune systems of vertebrates would lead to a better understanding of its biology, and possibly lead to a better understanding of PD etiology and pathogenesis. Hence, recent articles have studied aSyn for its potential involvement in anti-microbial defences. As such, the goal of the present study was to further investigate the possible anti-viral properties of aSyn, including differences amongst mutated forms of the protein, as well as its consequences following viral infections.

The effects of alpha-synuclein on viral infection

Previous results published by Park *et al* (2016) have demonstrated that aSyn confers anti-bacterial properties against *Escherichia coli, Pseudomonas aeruginosa, Staphylococcus epidermidis* and *Staphylococcus aureus* – bacterial strains know to cause infection in humans. By further investigating how aSyn limits the survival of bacterial strains (i.e. *Escherichia coli*), Park *et al* treated *Escherichia coli* cells with a fluorescent green dye which is unable to penetrate live-cell membranes. After the addition of aSyn, increases in fluorescent signal were observed with increasing concentrations of added protein, suggesting that the membranolytic action of aSyn led to E. coli cell death. From their findings, they suggested that aSyn may play a role within the innate immune system as a defense molecule. Not only has aSyn been implemented as an anti-bacterial protein, but also as an anti-viral protein. Previous results published by our lab have demonstrated that aSyn conferred better survival of newborn mice injected with reovirus T3D than *Snca* knockout mice (Tomlinson *et al,* 2017). Additionally, a previous member of our lab – Chris Rousso - found that aSyn (including WT and mutant forms of the protein) conferred

protective properties against VSV-GFP infection in H4 neuroglioma cells in a protein-dose dependant manner (Rousso, 2019). To note, these results have not been peer reviewed but are documented in a Master's thesis.

To further investigate how different forms of this protein effect the viral infectivity of cells, additional aSyn mutations were investigated following similar paradigms to that previously established by Chris Rousso (2019). PD-linked mutations A53T, A30P, E46K, and G51D were studied along with investigative mutations S129A, d119 and 3xA-P. The PD-linked mutations utilized in this study have all been implemented with early disease onset and disease pathogenesis (Srinivasan *et al,* 2021). While not genomically found in PD patients, the additional mutations used in this study have been created with the intention of altering the protein's metabolism to investigate the role of specific features, such as phosphorylation at serine 129 as well as to facilitate its aggregation. By substituting the serine for an alanine at amino acid 129, the process of phosphorylation is blocked at this location. This is an important investigative tool considering that almost all aggregated aSyn found in Lewy bodies of PD patients is phosphorylated at this site (Anderson *et al,* 2006; Mavroudis *et al,* 2020). Additionally, the truncation of aSyn at amino acid 119 (d119) removes this site completely and also mimics truncated forms of aSyn occasionally found in PD patients. Finally, the 3xA-P mutation substitutes three alanines with prolines. The added proline acids to the protein sequence should ideally increase the protein's propensity to oligomerize (Bergdoll et al, 1997); thus, it could serve as a useful tool when studying the effects of viral infections on aSyn metabolism as evaluated in later aims.

To investigate how these various mutations of aSyn affect VSV-GFP infection in cells, the different aSyn constructs were propagated and transfected into H4 neuroglioma cells and

subsequently infected with a low MOI (0.1) of VSV-GFP for 20 hours. The MOI and length of infection were chosen to best promote viral replication without inducing cell death. After infection with VSV-GFP, fluorescent quantification of the total number of GFP-positive cells was performed to understand how aSyn could affect the replication of the virus. Through a combination of fluorescent microscopy and flow cytometry, I found that aSyn – WT or mutated – did not significantly affect viral replication within the cells compared to the respective vector controls (**figures 6-11**). Of note, fluorescent quantification was the chosen readout of this project, and as a consequence plaque assays to confirm viral load/replication (via plaque forming units) were not conducted but could be utilized in future experiments to strengthen the findings. While the results were not statistically significant, certain trends indicative of a protective function of aSyn between replicated experimental runs were observed. When comparing each mutation to WT aSyn, some assumptions could be made regarding the possible protective effect of each mutation. Through fluorescent analysis, mutations A30P, A53T and E46K appeared to decrease the number of GFP-positive cells less effectively than WT aSyn (**figures 6-9**). In contrast, mutations G51D, S129A, d119 and 3xA-P all seemed to influence the number of GFP-positive cells in an equal manner to WT aSyn, often reducing the number of GFP-positive cells similarly to (and sometimes greater than) WT aSyn transfected cells (**figures 7-9**).

The trends observed in cells transfected with the A30P, A53T and E46K mutations were mostly expected. Following the work conducted by Chris Rousso (2019), both A53T and E46K mutations were expected to marginally protect H4 cells against VSV-GFP infection, to a lesser extent than WT aSyn. It was also expected that the A30P mutation would marginally protect the cells from infection, if at all. This assumption follows the reasoning that the alanine to proline substitution could increase the protein's potential to oligomerize, and thus increase the likelihood

of protein aggregation (Hashimoto and Panchenko, 2010). The observations using G51D mutated aSyn were somewhat unexpected. Aspartic acid (D) is known to undergo the post- translational modification of isomerization (Yi *et al,* 2023). Isomerization is the process in which the protein backbone structure is altered, often resulting in changes in protein function. Additionally, the G51D mutation has been linked to early PD onset and the formation of aSyn oligomers and toxic fibrils (Lesage *et al,* 2013). It has been proposed the oligomeric species of aSyn could be a major source of cell toxicity (Xu *et al,* 2022). Of note, oligomers of mutated aSyn, including of the G51D mutant, can augment the rate of beta-sheet formation. These formations are implemented in both increased oligomerization and fibrilization, and thus increased aSyn aggregation (Xu *et al,* 2022). As such, it was unexpected that the G51D mutation would confer equivalent/increased cell protection against VSV-GFP compared to the WT aSyn. Yet, this trend was observed across each experimental replicate within each experimental readout (**figures 7-11**).

Similarly to the observations of the G51D mutation, the S129A, d119 and 3xA-P mutation all appeared to confer equivalent/increased cell protection against VSV-GFP compared to WT aSyn. Considering that phosphorylated aSyn constitutes the vast majority of aSyn species within the Lewy bodies of PD patients, the phosphorylation of aSyn could be considered to contribute to disease pathology. By blocking the most common phosphorylation site – amino acid 129 – it was expected that the protein may aid in cell protection against VSV-GFP more effectively than other variants of the protein. This assumption shows merit throughout each experimental replicate, where a decrease in the number of GFP-positive cells were observed compared to the vector control and often to WT aSyn (**figures 7-11**). In contrast, the 3xA-P mutation also appeared to decrease the total number of GFP-positive cells to a similar extent of WT aSyn. This was mostly unexpected given that the additional proline acids should lead to an

increase in oligomerization, which in turn should lead to an increased propensity for the formation of aggregates. It is possible that the mutation is not increasing oligomerization as expected, considering that analyses observed via Western blot did not reveal any higher molecular weight protein species (**figures 12-13**). That being said, no higher molecular weight species of aSyn were observed on Western blots of any of the tested mutations, and therefore does not prove or disprove the presence of aSyn oligomers. From another perspective, the protective effects observed in the 3xA-P mutation could in part be due to the vast inconsistencies of observable GFP-positive cells between experimental replicates. While conducting the experiments in H4 cells, variability was evident in the percentage of GFP-positive cells amongst many of the tested constructs. This variability was most evidently seen in the vector controls (**figures 3 and 4**).

To overcome this variability issue, numerous troubleshooting and optimization steps were taken. Firstly, the conditions of the experiment were re-optimized to confirm the best suited conditions for the desired outcome were being used. The MOI of VSV-GFP used was optimized again, using cell transfected with only the vector controls incorporated in the study (pcDNA31, empty vector control and pDEST empty vector control) to determine how reproducible the results were. This step confirmed that large variability between replicated experiments existed when performed under the same conditions (**figure 4**). When discussing the results with the lab's adjunct virologist, Dr. Earl Brown, a better system for infecting cells was proposed and implemented. Prior to this discussion, time zero of infection was documented as the moment VSV-GFP was introduced to the cells with the addition of culture media. This protocol was adapted to allow the cells 30 minutes to take-up the virus before the official infection start time (time zero) was recorded. This step was incorporated to allow for a more accurate infection

process, however, did not reduce the variability seen in the results. From here, different durations of infection were tested using the newly adapted protocol to confirm that the best conditions were being utilized to test the desired aim. It was decided, still, that a 20-hour infection period with a MOI of 0.1 was sufficient to infect the majority of untransfected cells, without inducing major cell death.

After redefining and confirming that the experimental design was optimal to test my experimental aim, the plasmids themselves were studied as the reason for result variabilities. Each aSyn constructed employed in the study was sequenced in triplicate to ensure that the desired mutation was present, and that the empty vector controls did not have an inserted sequence that was being transcribed during transfection. Each construct and control were in fact what they were thought to be. Because there was no gene being transcribed in the empty vector controls, the purity of the plasmid preparations was viewed via gel electrophoresis. On a 0.8% agarose gel, each plasmid used in the study showed no DNA contamination. Therefore, the purity of the plasmid preparations was not thought to be a cause for the inconsistencies seen in the results. However, to test whether additional contaminants were present within the plasmid DNA, further analysis using LPS was conducted (**Figure 5**). We hypothesised that, perhaps, contaminants within the expression plasmids were inducing an interferon response via innate antiviral pathways, thereby impairing the infectivity of the VSV-GFP virus. To address this, LPS was used to treat cells independent of VSV-GFP infection. Since LPS is a bacterial toxin capable of invoking an interferon response, if the presence of interferons were the reason for GFP-signal inconsistencies then there should exist inconsistencies between LPS treated cells as well. However, there was no evidence of altered VSV-GFP infection (as determined via GFP fluorescence) in LPS treated cells. Considering that LPS treated cells, and completely

untransfected/untreated cells, showed no variations in detectable GFP-signal, the infection efficiency of the VSV-GFP virus was not considered a reason for variability in the experimental results. It must be noted that experimental limitations existed. For example, the cells could have been treated directly with interferons to act as a positive control when assessing the innate anti-viral response to further confirm the findings of LPS-treated cells.

Finally, we hypothesized that CMV promoter competition could be the reason for the observed variability, such as that during the process of transcription initiation, when RNA polymerases are recruited to a promoter site, the lack of a transcribable sequence (within the vector control plasmid construct) could paradoxically cause polymerases to be recruited (but without actively transcribing nucleotide sequences). Thus, they are unable to be recruited for engaging start codons within the VSV-GFP virus-encoded sequence during infection, which is required for efficient viral replication. To test this theory, a new cDNA construct was introduced, i.e.., encoding for gamma-synuclein (gSyn), because this synuclein family member has not been implemented in PD- or dementia-associated Lewy body disorders and is not currently considered a pathological hallmark of disease. That said, the reason for incorporating it in the study was to have a cDNA other that *SNCA* to be encoded, in an attempt to address the theory of promoter competition. Nevertheless, inconsistencies were observed with that control in place as well, namely in the percentage of observed GFP-signal produced by gSyn transfected cells from experiment to experiment. This suggested to us that promoter competition was not the cause for the variability observed. From here, we propose that the variability is likely attributed to other cell biological events and most likely to the utilization of transiently transfected cells (Langereis *et al,* 2015). This prompted me to move into another cell model to continue testing my aim.

By using an already established stable cell line (PC12-C4) that overexpresses human WT aSyn in an inducible system, I was able to test my initial aim in the context of WT aSyn; however, I was unable to evaluate differences between aSyn mutations. The PC12-C4 cell model works as a Tet-off system, where aSyn expression can be silenced in the presence of doxycycline (PC12-C4 +dox), but under normal conditions the overexpression of aSyn remains (PC12-C4 -dox). As a control for the effects of doxycycline on the cells, parental PC12 cells which do no express human *SNCA* cDNA, were used. By removing the need to transiently transfect cells, this seemed to be a suitable model to test whether WT aSyn could induce an anti-viral effect during VSV-GFP infection. VSV-GFP infections in PC12-C4 and PC12 cells were optimized to a MOI of 3.0 for three hours. These cells were much more susceptible to infection than the H4 cells previously studied. As such, a shorter duration infection was required to avoid cell death. To combat the shorter infection period, a higher MOI was optimized to still cause high rates of infection. Similarly to the experimental readouts utilized in the H4 cell model, fluorescent microscopy and flow cytometry analysis were conducted to quantify the total number of GFP-positive cells following infection.

In both experimental readouts, cells which overexpressed human aSyn did not confer any protective qualities against VSV-GFP infection compared to cells that expressed no human aSyn (**figures 14 and 15**). This was unexpected given the ample evidence to support that aSyn possesses anti-microbial properties. Similarly, Western blot analyses revealed no alterations in VSV protein levels when aSyn was either overexpressed or silenced, complementing the results seen in fluorescent analyses (**figure 16**). Together, the findings from this experimental model suggest that WT aSyn does not protect PC12-C4 cells from VSV-GFP infection. However, it could be possible that the endogenous rat *Snca* within PC12-C4 cells already produces enough

aSyn to observe the full anti-viral potential of the protein, and that the addition of overexpressed human aSyn does not increase this response further. Additional studies could be incorporated by knocking out the rat *Snca* gene in these cells to further examine this possibility. It must also be noted that other limitations in this model exist. For example, the sensitivity of the cells to infection may indicate that this virus and cell model are not ideal for testing my aim. In fact, even with such a short infection period, cell death was observed which could influence the results. It would be beneficial to test this aim in a similar manner using another viral pathogen to strengthen the conclusion that, in theses cells, WT aSyn does not provide protection against viral infection.

Consequences of aSyn following viral infection

While the initial aim of this study was to determine the effects that aSyn, including WT and mutated forms, had on a viral infection, the secondary aim was to investigate what happens to aSyn itself following infection. Previous studies have shown that aSyn can undergo conformational changes leading to its aggregation following different microbial infections. One study conducted by Huynh *et al,* (2023) utilized a *Caenorhabditis elegans* model to investigate whether bacterial strains of *Desulfovibrio* bacteria isolated from PD patients could induce aSyn aggregation, compared to bacteria isolated from healthy controls. Their results indicate that aSyn aggregation was significantly increased in *Caenorhabditis elegans* that consumed the PD patient bacteria in comparison to worms that were fed the control bacteria strains. Of note, the size of these aggregates was also greatly increased (Huynh *et al,* 2023). While their results do not directly define whether bacteria isolated from PD patients were pathogenic or not, their results suggested that worms fed the PD patient-derived bacteria had a decreased survival. Further analysis of the bacteria itself should be completed to inform what possible changes could be

altering it into a pathogenic state. Overall, this study confers that certain bacterial strains can induce alterations in aSyn metabolism (Huynh *et al,* 2023). Similar changes in aSyn have also been observed following select viral infections. A recent study conducted by Limanaqi *et al* (2024) demonstrated that aSyn undergoes conformational changes (specifically the formation of non-toxic multimers) following SARS-CoV-2 infections. Using various cell models (i.e. epithelial lung cell lines, umbilical vein endothelial cells, and peripheral blood mononuclear cells) they observed both the promotion of these multimeric aSyn species and inhibited viral replication upon the addition of aSyn (Limanaqi *et al,* 2024). They proposed that these events likely occurred as a type-1 interferon-related response. All in all, ample evidence exists supporting the theory that microbial infections can induce metabolic changes in aSyn, including its conformation.

To further investigate how different forms of aSyn (including familial PD-linked mutations and additional investigative aSyn mutations) are affected following viral infection, cell samples obtained from the experiments conducted to test the first aim were lysed and used in Western blot analyses against aSyn (using the antibody Syn1). First, changes in aSyn expression in VSV-GFP infected cells were compared to that of mock treated cells. It was expected that, if aSyn possessed anti-viral properties, it would be upregulated in the presence of the viral pathogen to aid in host defence and such upregulation should be detectable by Western blotting. In each of the tested cell lysates, no significant differences in the total protein expression were detected; however, there seemed to exist a trend indicating that the protein's expression is minimally downregulated post-infection (**figures 12 and 13**). These results were unexpected, considering the thought that aSyn – if protective – would likely become more rapidly produced to defend against the viral pathogen. Perhaps, reductions during the transcription/translation

phases could have decreased the amount of *SNCA* produced, thus limiting the amount of observable aSyn in experimental readouts. Alternatively, alterations in subcellular distribution could be rendering aSyn less visible in the extracted phases; however, the precise cause remains unknown. When examining the Western blots, a second goal was to observe any higher molecular weight species of aSyn, which would correlate with the presence of aSyn oligomers. Ideally, if the protein underwent conformational changes during infection, that could explain the appearance of downregulated protein levels as observed. However, no such species were observable on the blots (**figures 12 and 13**). This could indicate that 1) oligomerization is not happening as a result of infection, or 2) the ratio between oligomer and monomeric aSyn species remains too low to be observable under chemiluminescence. These results, together, were mostly unexpected considering that many of these mutations have previously been found to promote oligomerization and fibril formation. It must be remembered that variations in the data existed between experimental replicates in terms of GFP fluorescence. It could therefore be possible that variations in Western blot data exist, which could contribute to the inability to draw definitive conclusions from the data.

Similarly, the PC12-C4 cell model was utilized to support the hypothesis without the need for transient transfection. Western blot analyses against aSyn were conducted following the same paradigms as before. Again, aSyn protein expression was examined and compared between mock treated and VSV-GFP infected cell lysates. Similarly to the results seen in the H4 cell model, no significant changes in the steady-state of total aSyn were observed in PC12-C4 cells following infection compared to that of the mock treated cells (**figure 16**). Additionally, no higher molecular weight species of aSyn were observed on Western blots. It could be that the short infection duration (3 hours) was not sufficient to promote the production of oligomeric

species; however, further analysis would need to be conducted to prove/disprove this theory. Overall, even if not observable, the lack of higher molecular weight aSyn species of the Western blots does not definitively suggest that oligomerization is not happening. Therefore, to test whether the presence of aSyn oligomers increases in response to infection, additional readouts needed to be incorporated.

The lack of observable alterations in aSyn protein metabolism within the H4 and PC12-C4 cell models led to the pursuit of another model which does not solely rely on Western blot analysis to confer oligomeric species of aSyn. In such, a BiSyn construct was utilized in H4 cells. This BiSyn construct encodes two *SNCA* sequences, each containing part of a GFP sequence. One half of the GFP sequence is attached to the C-terminal end of the first *SNCA*, while the other GFP half is attached to the N-terminal end of the second *SNCA*. In theory, if the two aSyn products combined to form an oligomer, the GFP halves will come together and fluoresce. 24-hours after this construct was transfected into H4 cells, the cells were infected with wild-type VSV (MOI 0.5) for 24 hours, similarly to previous experiments conducted using this cell line. Through fluorescent microscopy, it was evident that the number of cells producing GFP was greatly increased in cells infected with VSV compared to cells which were not infected (**figure 17**). Further, Western blot analysis conferred that the total amount of aSyn expression in both infected and mock treated cells was equivalent. This suggested that, while the total amount of aSyn expression stayed consistent, the formation of oligomeric aSyn increased in response to infection. It must be noted, however, that aSyn oligomerization is observed in mock-treated cell at a lesser extent. Still, the results observed were as hypothesized; aSyn did indeed appear to undergo alterations following infection. Next, the time at which rapid oligomerization began within the infected cells was observed via live-cell imaging. Time-lapse videos of cells infected

with increased MOIs of VSV, and mock treated cells were captured over the course of 21 hours. Still images were taken from these videos for the purpose of this report from each tested condition (**figure 18**). While aSyn di-/oligomers are still observable in the mock treated cells, they appeared to form at both a faster rate and with a higher propensity when the cells were infected with VSV. Taken together, these results indicate that viral infection can initiate changes in aSyn metabolism and promote protein aggregation. While still preliminary, the results using the BiSyn are quite compelling. Further studies utilizing this construct within additional cell models, including primary neuronal cultures, should be conducted to show reproducibility and strengthen the evidence suggested in this study. Also, it would be beneficial to conduct similar studies which utilize different microbial pathogens, including both bacterial pathogens and viruses. Bacterial strains such as *Staphylococcus aureus* could be of interest as it could bridge the relationship between the nasal/olfactory system (which has been implemented in the dule hit hypothesis) and aSyn accumulation. Additionally, further studies utilizing SARS-CoV-2 and influenza subtypes known to cause infection in humans could be of interest. Of note, our lab recently established that – in some instances – fatal cases of SARS-CoV-2 reflected occurrences of neurodegeneration within the olfactory bulb which mimicked neurodegenerative processes seen in other brain regions (Lengacher *et al,* 2023). The addition of such viruses would not only demonstrate reproducibility of results in related paradigms, but aid in further strengthening the argument that aSyn is implemented within the innate immune system. Of note, this BiSyn construct only allows the for the investigation of WT aSyn. Additional constructs could be created using a similar structure to incorporate different mutations of aSyn to be utilized in similar studies.

Chapter 5. Conclusion

The aim of the present study was to investigate how aSyn behaves in the presence of a concrete microbial pathogen, VSV, and what implications viral infections may have on the protein itself. Throughout the study, a protective role of aSyn against VSV infection was not observed with statistical significance within the model systems tested. Yet, differences in potential anti-viral affects between different aSyn species were observed. At this time, limitations and variability of the data do not allow for definitive conclusions to be drawn. In contrast, the data do suggest that aSyn undergoes metabolic changes following viral infection, including changes in its conformation. Taken together, the results suggest that certain viral pathogens could potentially lead to the changes in aSyn's behaviour, including the promotion of its aggregation, which is seen in PD tissues. Further studies to confirm these finding, and further investigations into the role that aSyn plays during infection, should be conducted to better define the functions of aSyn within the immune system. Additionally, incorporating other types of microbial pathogens (bacterial, other RNA viruses, DNA viruses, *etc*.) could help uncover how different infections could elicit different responses by / functions of aSyn. Replicating similar studies in different cell models, such as primary neurons, IPSC, glial cells and organoids as well as in vivo models, could lead to a better understanding of aSyn biology, and in turn would help shed light on aspects of PD pathogenesis. Overall, this study sheds light on how microbial triggers may initiate the changes in aSyn that are observed in PD.

Appendix 1

Table 1. Summary of troubleshooting steps taken to overcome data inconsistencies observed within the H4 transient transfection experiments.

Step Taken	Goal(s)	Outcome(s)
Further optimization	Optimization of VSV-GFP MOI Optimization of amount of DNA to transfect into H4 cells	MOI 0.1 sufficient for desired study 0.5µg of plasmid DNA efficiently transfected the cells
Protocol adaptations	Establish a better system of infecting cells with VSV-GFP	Suggestions by Dr. Earl Brown led to adaptations in the infection protocol to ensure proper infection of cells
Cell fixation with 0.4% PFA	To minimize lifting cells during microscopy	Fixation did not interfere with GFP-signal, and stopped the cells from lifting off the plate surface during imaging
Indirect immunofluorescence	To see if differences in GFP-signal are observed in comparison to direct fluorescent microscopy	No changes were observed.
Time-course analysis	To observe the best duration of infection to use for the purpose of this study	20 hours, rather than 24, allowed for the optimal measure of GFP-positive cells while minimizing cell death
Analysis of culture media	To confirm accurate pH of cell culture media	Cell culture media has the desired pH and is not concluded to cause data variability
Plasmid DNA sequencing	To confirm each plasmid sequence is as expected	Each plasmid sequence was as expected
Visualization of plasmid DNA	To visualize any contaminants within the DNA preparations	No contaminants were observed, and DNA was in-tact
Minipreps of plasmid DNA	To allow for higher yield of plasmid DNA in comparison to maxiprepped DNA	Minipreps allowed for a higher concentration of DNA
Implementation of lipofectamine2000 control	To ensure infection efficiency is consistent in untransfected cells	Untransfected cells (treated with L2000) consistently showed full infection of VSV-GFP
LPS treatment	To see if interferon responses could be hindering VSV-GFP replication	Treatment with LPS did not alter the infectivity of cells compared to untransfected cells

References

Adler, C.H., Connor, D.J., Hentz, J.G., Sabbagh, M.N., Caviness, J.N., Shill, H.A., Noble, B. and Beach, T.G. (2010). Incidental Lewy Body disease: Clinical Comparison to a Control Cohort. *Movement Disorders*, 25(5), pp.642–646. doi:https://doi.org/10.1002/mds.22971.

Alam, Md Masud, et al. "Alpha Synuclein, the Culprit in Parkinson Disease, Is Required for Normal Immune Function." *Cell Reports*, vol. 38, no. 2, Jan. 2022, p. 110090, https://doi.org/10.1016/j.celrep.2021.110090.

Allen Reish, Heather E., and David G. Standaert. "Role of α-Synuclein in Inducing Innate and Adaptive Immunity in Parkinson Disease." *Journal of Parkinson's Disease*, vol. 5, no. 1, 2015, pp. 1–19, https://doi.org/10.3233/jpd-140491.

Ana Martinez Hernandez, et al. "Low-Expressing Synucleinopathy Mouse Models Based on Oligomer-Forming Mutations and C-Terminal Truncation of α-Synuclein." *Frontiers in Neuroscience*, vol. 15, 17 June 2021, https://doi.org/10.3389/fnins.2021.643391.

Anderson, J.P., Walker, D.E., Goldstein, J.M., de Laat, R., Banducci, K., Caccavello, R.J., Barbour, R., Huang, J., Kling, K., Lee, M., Diep, L., Keim, P.S., Shen, X., Chataway, T., Schlossmacher, M.G., Seubert, P., Schenk, D., Sinha, S., Gai, W.P. and Chilcote, T.J. (2006). Phosphorylation of Ser-129 Is the Dominant Pathological Modification of α-Synuclein in Familial and Sporadic Lewy Body Disease. *Journal of Biological Chemistry*, 281(40), pp.29739–29752. doi:https://doi.org/10.1074/jbc.m600933200.

Azeredo da Silveira, Samareh, et al. "Phosphorylation Does Not Prompt, nor Prevent, the Formation of Alpha-Synuclein Toxic Species in a Rat Model of Parkinson's Disease." *Human Molecular Genetics*, vol. 18, no. 5, 1 Mar. 2009, pp. 872–887, https://doi.org/10.1093/hmg/ddn417.

Beatman, Erica L., et al. “Alpha-Synuclein Expression Restricts RNA Viral Infections in the Brain.” *Journal of Virology*, vol. 90, no. 6, 15 Mar. 2016, pp. 2767–2782, https://doi.org/10.1128/jvi.02949-15.

Bergdoll, Marc, et al. “Proline-Dependent Oligomerization with Arm Exchange.” *Structure*, vol. 5, no. 3, Mar. 1997, pp. 391–401, https://doi.org/10.1016/s0969-2126(97)00196-2.

Birkmayer, W., and O. Hornykiewicz. “[the L-3,4-Dioxyphenylalanine (DOPA)-Effect in Parkinson-Akinesia].” *Wiener Klinische Wochenschrift*, vol. 73, 10 Nov. 1961, pp. 787–788.

Bisi, Nicolò, et al. “α-Synuclein: An All-Inclusive Trip around Its Structure, Influencing Factors and Applied Techniques.” *Frontiers in Chemistry*, vol. 9, 7 July 2021, https://doi.org/10.3389/fchem.2021.666585.

Borghammer, Per, and Nathalie Van Den Berge. “Brain-First versus Gut-First Parkinson’s Disease: A Hypothesis.” *Journal of Parkinson’s Disease*, vol. 9, no. s2, 30 Oct. 2019, pp. S281–S295, https://doi.org/10.3233/jpd-191721.

Braak, Heiko, et al. “Staging of Brain Pathology Related to Sporadic Parkinson’s Disease.” *Neurobiology of Aging*, vol. 24, no. 2, Mar. 2003, pp. 197–211, https://doi.org/10.1016/s0197-4580(02)00065-9.

Brown, Jennifer L, et al. “*SNCA* Genetic Lowering Reveals Differential Cognitive Function of Alpha-Synuclein Dependent on Sex.” *Acta Neuropathologica Communications*, vol. 10, no. 1, 14 Dec. 2022, https://doi.org/10.1186/s40478-022-01480-y.

Brundin, Patrik, and Ronald Melki. “Prying into the Prion Hypothesis for Parkinson’s Disease.” *The Journal of Neuroscience*, vol. 37, no. 41, 11 Oct. 2017, pp. 9808–9818, https://doi.org/10.1523/jneurosci.1788-16.2017.

Burke, Robert E, et al. “A Critical Evaluation of the Braak Staging Scheme for Parkinson’s Disease.” *Annals of Neurology*, vol. 64, no. 5, 2008, pp. 485–91, https://doi.org/10.1002/ana.21541.

Burre, J., et al. “ -Synuclein Promotes SNARE-Complex Assembly in Vivo and in Vitro.” *Science*, vol. 329, no. 5999, 26 Aug. 2010, pp. 1663–1667, https://doi.org/10.1126/science.1195227.

Burré, Jacqueline, et al. “Cell Biology and Pathophysiology of α-Synuclein.” *Cold Spring Harbor Perspectives in Medicine*, vol. 8, no. 3, 20 Jan. 2017, p. a024091, https://doi.org/10.1101/cshperspect.a024091.

Chahine, Lana M, et al. “Proposal for a Biologic Staging System of Parkinson’s Disease.” *Journal of Parkinson’s Disease*, 10 Apr. 2023, pp. 1–13, https://doi.org/10.3233/jpd-225111.

Chang, Diana, et al. “A Meta-Analysis of Genome-Wide Association Studies Identifies 17 New Parkinson’s Disease Risk Loci.” *Nature Genetics*, vol. 49, no. 10, 11 Sept. 2017, pp. 1511–1516, https://doi.org/10.1038/ng.3955.

Chen, Merry, and Danielle Emille Mor. “Gut-To-Brain α-Synuclein Transmission in Parkinson’s Disease: Evidence for Prion-like Mechanisms.” *International Journal of Molecular Sciences*, vol. 24, no. 8, 13 Apr. 2023, pp. 7205–7205, https://doi.org/10.3390/ijms24087205.

Chia, Shyh Jenn, et al. “Historical Perspective: Models of Parkinson’s Disease.” *International Journal of Molecular Sciences*, vol. 21, no. 7, 2 Apr. 2020, p. 2464, https://doi.org/10.3390/ijms21072464.

Cocoros, Noelle M., et al. “Long-Term Risk of Parkinson Disease Following Influenza and

Other Infections." *JAMA Neurology*, 25 Oct. 2021, https://doi.org/10.1001/jamaneurol.2021.3895.

Colla, Emanuela, et al. "Subcellular Localization of Alpha-Synuclein Aggregates and Their Interaction with Membranes." *Neural Regeneration Research*, vol. 13, no. 7, 9 May 2018, p. 1136, https://doi.org/10.4103/1673-5374.235013.

Coon, Elizabeth A., and Wolfgang Singer. "Synucleinopathies." *CONTINUUM: Lifelong Learning in Neurology*, vol. 26, no. 1, Feb. 2020, pp. 72–92, https://doi.org/10.1212/con.0000000000000819.

Cullen, Valerie, et al. "Cathepsin D Expression Level Affects Alpha-Synuclein Processing, Aggregation, and Toxicity in Vivo." *Molecular Brain*, vol. 2, no. 1, 2009, p. 5, https://doi.org/10.1186/1756-6606-2-5.

Dordevic, D, et al. "Hydrogen Sulfide Toxicity in the Gut Environment: Meta-Analysis of Sulfate-Reducing and Lactic Acid Bacteria in Inflammatory Processes." *Journal of Advanced Research*, 17 Mar. 2020, https://doi.org/10.1016/j.jare.2020.03.003.

Emmi, Aron, et al. "Smell Deficits in COVID-19 and Possible Links with Parkinson's Disease." *International Review of Neurobiology*, 1 Jan. 2022, pp. 91–102, https://doi.org/10.1016/bs.irn.2022.08.001.

Esteves, A. Raquel, et al. "LPS-Induced Mitochondrial Dysfunction Regulates Innate Immunity Activation and α-Synuclein Oligomerization in Parkinson's Disease." *Redox Biology*, vol. 63, 1 July 2023, p. 102714, https://doi.org/10.1016/j.redox.2023.102714.

Fu, Yajuan, et al. "Inhibition of CGAS-Mediated Interferon Response Facilitates Transgene Expression." *IScience*, vol. 23, no. 4, 31 Mar. 2020, p. 101026, https://doi.org/10.1016/j.isci.2020.101026.

Gardai, Shyra J., et al. “Elevated Alpha-Synuclein Impairs Innate Immune Cell Function and Provides a Potential Peripheral Biomarker for Parkinson’s Disease.” *PLoS ONE*, vol. 8, no. 8, 23 Aug. 2013, p. e71634, https://doi.org/10.1371/journal.pone.0071634.

Ghanem, Simona S, et al. “α-Synuclein Phosphorylation at Serine 129 Occurs after Initial Protein Deposition and Inhibits Seeded Fibril Formation and Toxicity.” *Proceedings of the National Academy of Sciences of the United States of America*, vol. 119, no. 15, 30 Mar. 2022, https://doi.org/10.1073/pnas.2109617119.

Goetz, C. G. “The History of Parkinson’s Disease: Early Clinical Descriptions and Neurological Therapies.” *Cold Spring Harbor Perspectives in Medicine*, vol. 1, no. 1, 1 Sept. 2011, https://doi.org/10.1101/cshperspect.a008862.

Grotemeyer, Alexander, et al. “Inflammasome Inhibition Protects Dopaminergic Neurons from α-Synuclein Pathology in a Model of Progressive Parkinson’s Disease.” *Journal of Neuroinflammation*, vol. 20, no. 1, 21 Mar. 2023, p. 79, https://doi.org/10.1186/s12974-023-02759-0.

Hashimoto, K., and A. R. Panchenko. “Mechanisms of Protein Oligomerization, the Critical Role of Insertions and Deletions in Maintaining Different Oligomeric States.” *Proceedings of the National Academy of Sciences*, vol. 107, no. 47, 3 Nov. 2010, pp. 20352–20357, https://doi.org/10.1073/pnas.1012999107.

Hirsch, Lauren, et al. “The Incidence of Parkinson’s Disease: A Systematic Review and Meta-Analysis.” *Neuroepidemiology*, vol. 46, no. 4, 2016, pp. 292–300, https://doi.org/10.1159/000445751.

Hoffman, Leslie A, and Joel A Vilensky. “Encephalitis Lethargica: 100 Years after the Epidemic.” *Brain*, vol. 140, no. 8, 14 July 2017, pp. 2246–2251,

https://doi.org/10.1093/brain/awx177.

Holmqvist, Staffan, et al. “Direct Evidence of Parkinson Pathology Spread from the Gastrointestinal Tract to the Brain in Rats.” *Acta Neuropathologica*, vol. 128, no. 6, 9 Oct. 2014, pp. 805–820, https://doi.org/10.1007/s00401-014-1343-6.

Huynh, Vy A, et al. “Desulfovibrio Bacteria Enhance Alpha-Synuclein Aggregation in a Caenorhabditis Elegans Model of Parkinson’s Disease.” *Frontiers in Cellular and Infection Microbiology*, vol. 13, 1 May 2023, https://doi.org/10.3389/fcimb.2023.1181315.

Jagadeesan, A. J., et al. “Current Trends in Etiology, Prognosis and Therapeutic Aspects of Parkinson’s Disease: A Review.” *Acta Bio-Medica: Atenei Parmensis*, vol. 88, no. 3, 23 Oct. 2017, pp. 249–262, https://doi.org/10.23750/abm.v88i3.6063.

Jan, Asad, et al. “The Prion-like Spreading of Alpha-Synuclein in Parkinson’s Disease: Update on Models and Hypotheses.” *International Journal of Molecular Sciences*, vol. 22, no. 15, 3 Aug. 2021, p. 8338, https://doi.org/10.3390/ijms22158338.

Jang, Haeman, et al. “Viral Parkinsonism.” *Biochimica et Biophysica Acta*, vol. 1792, no. 7, 1 July 2009, pp. 714–721, https://doi.org/10.1016/j.bbadis.2008.08.001.

Jankovic, J. “Parkinson’s Disease: Clinical Features and Diagnosis.” *Journal of Neurology, Neurosurgery & Psychiatry*, vol. 79, no. 4, 1 Apr. 2008, pp. 368–376, https://doi.org/10.1136/jnnp.2007.131045.

Kalia, L. V., & Lang, A. E. “Parkinson’s disease”. *The Lancet*. 2015. https://doi.org/https://doi.org/10.1016/S0140-6736(14)61393-3

Kasen, Alysa, et al. “Upregulation of α-Synuclein Following Immune Activation: Possible Trigger of Parkinson’s Disease.” *Neurobiology of Disease*, vol. 166, 1 May 2022, p.

105654, https://doi.org/10.1016/j.nbd.2022.105654.

Kawahata, Ichiro, et al. “Pathogenic Impact of α-Synuclein Phosphorylation and Its Kinases in α-Synucleinopathies.” *International Journal of Molecular Sciences*, vol. 23, no. 11, 1 Jan. 2022, p. 6216, https://doi.org/10.3390/ijms23116216.

Klein, C., and A. Westenberger. “Genetics of Parkinson’s Disease.” *Cold Spring Harbor Perspectives in Medicine*, vol. 2, no. 1, 1 Jan. 2012, pp. a008888–a008888, https://doi.org/10.1101/cshperspect.a008888.

Koga, Shunsuke, et al. “Neuropathology and Molecular Diagnosis of Synucleinopathies.” *Molecular Neurodegeneration*, vol. 16, no. 1, Dec. 2021, https://doi.org/10.1186/s13024-021-00501-z.

Kordower, Jeffrey H, et al. “Lewy Body–like Pathology in Long-Term Embryonic Nigral Transplants in Parkinson’s Disease.” *Nature Medicine*, vol. 14, no. 5, 6 Apr. 2008, pp. 504–506, https://doi.org/10.1038/nm1747.

Kouli, Antonina, et al. “Parkinson’s Disease: Etiology, Neuropathology, and Pathogenesis.” *Parkinson’s Disease: Pathogenesis and Clinical Aspects*, vol. 1, no. 1, 22 Dec. 2018, pp. 3–26, https://doi.org/10.15586/codonpublications.parkinsonsdisease.2018.ch1.

Langereis, Martijn A., et al. “Knockout of CGAS and STING Rescues Virus Infection of Plasmid DNA-Transfected Cells.” *Journal of Virology*, vol. 89, no. 21, 1 Nov. 2015, pp. 11169–11173, https://doi.org/10.1128/JVI.01781-15.

Lei, Zhinian, et al. “A30P Mutant α-Synuclein Impairs Autophagic Flux by Inactivating JNK Signaling to Enhance ZKSCAN3 Activity in Midbrain Dopaminergic Neurons.” *Cell Death & Disease*, vol. 10, no. 2, Feb. 2019, https://doi.org/10.1038/s41419-019-1364-0.

Lengacher, N.A., Tomlinson, J.J., Jochum, A.-K., Franz, J., Ali, O.H., Flatz, L., Jochum, W.,

Penninger, J., aSCENT-PD Investigators, Stadelmann-Nessler, C., Woulfe, J.M. and Schlossmacher, M.G. (2023). Neuropathological Assessment of the Olfactory Bulb and Tract in Individuals with COVID-19. *Semantic Scholar*. doi:https://doi.org/10.1101/2023.12.18.572180.

Lesage, Suzanne, et al. "G51D α-Synuclein Mutation Causes a Novel Parkinsonian-Pyramidal Syndrome." *Annals of Neurology*, vol. 73, no. 4, Apr. 2013, pp. 459–471, https://doi.org/10.1002/ana.23894.

Leta, Valentina, et al. "Viruses, Parkinsonism and Parkinson's Disease: The Past, Present and Future." *Journal of Neural Transmission*, vol. 129, no. 9, 29 Aug. 2022, pp. 1119–1132, https://doi.org/10.1007/s00702-022-02536-y.

Lovley, D R, et al. "Reduction of Uranium by Cytochrome C3 of Desulfovibrio Vulgaris." *Applied and Environmental Microbiology*, vol. 59, no. 11, Nov. 1993, pp. 3572–3576, https://doi.org/10.1128/aem.59.11.3572-3576.1993.

Marras, C., et al. "Prevalence of Parkinson's Disease across North America." *Npj Parkinson's Disease*, vol. 4, no. 1, 10 July 2018, https://doi.org/10.1038/s41531-018-0058-0.

Marreiros, Rita, et al. "Disruption of Cellular Proteostasis by H1N1 Influenza a Virus Causes α-Synuclein Aggregation." *Proceedings of the National Academy of Sciences*, vol. 117, no. 12, 9 Mar. 2020, pp. 6741–6751, https://doi.org/10.1073/pnas.1906466117.

Mavroudis, Ioannis, et al. "Alpha-Synuclein Levels in the Differential Diagnosis of Lewy Bodies Dementia and Other Neurodegenerative Disorders." *Alzheimer Disease & Associated Disorders*, Apr. 2020, p. 1, https://doi.org/10.1097/wad.0000000000000381.

McFarland, Nikolaus R., et al. "α-Synuclein S129 Phosphorylation Mutants Do Not Alter Nigrostriatal Toxicity in a Rat Model of Parkinson Disease." *Journal of Neuropathology*

& Experimental Neurology, vol. 68, no. 5, May 2009, pp. 515–524, https://doi.org/10.1097/nen.0b013e3181a24b53.

Moors, Tim E., et al. "Multi-Platform Quantitation of Alpha-Synuclein Human Brain Proteoforms Suggests Disease-Specific Biochemical Profiles of Synucleinopathies." *Acta Neuropathologica Communications*, vol. 10, no. 1, 3 June 2022, https://doi.org/10.1186/s40478-022-01382-z.

Murros, Kari Erik. "Hydrogen Sulfide Produced by Gut Bacteria May Induce Parkinson's Disease." *Cells*, vol. 11, no. 6, 1 Jan. 2022, p. 978, https://doi.org/10.3390/cells11060978.

Niu, Mengyue, et al. "A Longitudinal Study on A-Synuclein in Plasma Neuronal Exosomes as a Biomarker for Parkinson's Disease Development and Progression." *European Journal of Neurology*, 9 Mar. 2020, https://doi.org/10.1111/ene.14208.

Ntetsika, Theodora, et al. "Novel Targeted Therapies for Parkinson's Disease." *Molecular Medicine*, vol. 27, no. 1, 25 Feb. 2021, https://doi.org/10.1186/s10020-021-00279-2.

Oueslati, Abid. "Implication of Alpha-Synuclein Phosphorylation at S129 in Synucleinopathies: What Have We Learned in the Last Decade?" *Journal of Parkinson's Disease*, vol. 6, no. 1, 30 Mar. 2016, pp. 39–51, https://doi.org/10.3233/jpd-160779.

Pandit, Esha, et al. "Single Point Mutations at the S129 Residue of α-Synuclein and Their Effect on Structure, Aggregation, and Neurotoxicity." *Frontiers in Chemistry*, vol. 11, 26 May 2023, https://doi.org/10.3389/fchem.2023.1145877.

Park, Seong-Cheol, et al. "Functional Characterization of Alpha-Synuclein Protein with Antimicrobial Activity." *Biochemical and Biophysical Research Communications*, vol. 478, no. 2, 16 Sept. 2016, pp. 924–928, https://doi.org/10.1016/j.bbrc.2016.08.052.

Parkinson, J. “An essay on the Shaking Palsy”. *Archives of Neurology*. 1969 https://doi.org/10.1001/archneur.1969.00480100117017

Pelzel-McCluskey, Angela, et al. “Review of Vesicular Stomatitis in the United States with Focus on 2019 and 2020 Outbreaks.” *Pathogens*, vol. 10, no. 8, 6 Aug. 2021, p. 993, https://doi.org/10.3390/pathogens10080993.

Perni, Michele, et al. “Comparative Studies in the A30P and A53T α-Synuclein C. Elegans Strains to Investigate the Molecular Origins of Parkinson’s Disease.” *Frontiers in Cell and Developmental Biology*, vol. 9, 22 Mar. 2021, https://doi.org/10.3389/fcell.2021.552549.

Pinto-Costa, Rita, et al. “Overexpression-Induced α-Synuclein Brain Spreading.” *Neurotherapeutics*, 13 Dec. 2022, https://doi.org/10.1007/s13311-022-01332-6.

Ramalingam, N., Jin, S.-X., Moors, T.E., Fonseca-Ornelas, L., Shimanaka, K., Lei, S., Cam, H.P., Watson, A.H., Brontesi, L., Ding, L., Hacibaloglu, D.Y., Jiang, H., Choi, S.J., Kanter, E., Liu, L., Bartels, T., Nuber, S., Sulzer, D., Mosharov, E.V. and Chen, W.V. (2023). Dynamic Physiological α-synuclein S129 Phosphorylation Is Driven by Neuronal Activity. *npj Parkinson’s Disease*, 9(1). doi:https://doi.org/10.1038/s41531-023-00444-w.

Ramalingam, Nagendran, and Ulf Dettmer. “Temperature Is a Key Determinant of Alpha- and Beta-Synuclein Membrane Interactions in Neurons.” *Journal of Biological Chemistry*, vol. 296, Jan. 2021, p. 100271, https://doi.org/10.1016/j.jbc.2021.100271.

Rauschenberger, Lisa, et al. “Age-Dependent Neurodegeneration and Neuroinflammation in a Genetic A30P/A53T Double-Mutated α-Synuclein Mouse Model of Parkinson’s

Disease." *Neurobiology of Disease*, vol. 171, Sept. 2022, p. 105798, https://doi.org/10.1016/j.nbd.2022.105798.

Reyes, Juan F., et al. "Accumulation of Alpha-Synuclein within the Liver, Potential Role in the Clearance of Brain Pathology Associated with Parkinson's Disease." *Acta Neuropathologica Communications*, vol. 9, no. 1, 20 Mar. 2021, https://doi.org/10.1186/s40478-021-01136-3.

Rietdijk, Carmen D, et al. "Exploring Braak's Hypothesis of Parkinson's Disease." *Frontiers in Neurology*, vol. 8, no. 37, 2017, https://doi.org/10.3389/fneur.2017.00037.

Rodríguez-Losada, Noela, et al. "Overexpression of Alpha-Synuclein Promotes Both Cell Proliferation and Cell Toxicity in Human SH-SY5Y Neuroblastoma Cells." *Journal of Advanced Research*, vol. 23, May 2020, pp. 37–45, https://doi.org/10.1016/j.jare.2020.01.009.

Ruf, Viktoria C., et al. "Different Effects of α-Synuclein Mutants on Lipid Binding and Aggregation Detected by Single Molecule Fluorescence Spectroscopy and ThT Fluorescence-Based Measurements." *ACS Chemical Neuroscience*, vol. 10, no. 3, 20 Mar. 2019, pp. 1649–1659, https://doi.org/10.1021/acschemneuro.8b00579.

Sampson, Timothy R, et al. "A Gut Bacterial Amyloid Promotes α-Synuclein Aggregation and Motor Impairment in Mice." *ELife*, vol. 9, 11 Feb. 2020, https://doi.org/10.7554/elife.53111.

Sato, Hiroyasu, et al. "Authentically Phosphorylated α-Synuclein at Ser129 Accelerates Neurodegeneration in a Rat Model of Familial Parkinson's Disease." *The Journal of Neuroscience: The Official Journal of the Society for Neuroscience*, vol. 31, no. 46, 16 Nov. 2011, pp. 16884–16894, https://doi.org/10.1523/JNEUROSCI.3967-11.2011.

Schidlitzki, Alina, et al. “Double-Edged Effects of Venglustat on Behavior and Pathology in Mice Overexpressing α-Synuclein.” *Movement Disorders*, 12 Apr. 2023, https://doi.org/10.1002/mds.29398.

Shen, Si, et al. “The Role of Pathogens and Anti-Infective Agents in Parkinson’s Disease, from Etiology to Therapeutic Implications.” *Journal of Parkinson’s Disease*, vol. 12, no. 1, 21 Jan. 2022, pp. 27–44, https://doi.org/10.3233/jpd-212929.

Shin, E.-C., Cho, S.H., Lee, D.-K., Hur, M.-W., Seung Woon Paik, Jeon Han Park and Kim, J. (2000). Expression Patterns of α-Synuclein in Human Hematopoietic Cells and in Drosophila at Different Developmental Stages. *Molecules and Cells*, 10(1), pp.65–70. doi:https://doi.org/10.1007/s10059-000-0065-x.

Simon, David K., et al. “Parkinson Disease Epidemiology, Pathology, Genetics, and Pathophysiology.” *Clinics in Geriatric Medicine*, vol. 36, no. 1, Feb. 2020, pp. 1–12, https://doi.org/10.1016/j.cger.2019.08.002.

Smeyne, Richard J., et al. “Infection and Risk of Parkinson’s Disease.” *Journal of Parkinson’s Disease*, vol. 11, no. 1, 2 Feb. 2021, pp. 31–43, https://doi.org/10.3233/jpd-202279.

Srinivasan, E., et al. “Alpha-Synuclein Aggregation in Parkinson’s Disease.” *Frontiers in Medicine*, vol. 8, 18 Oct. 2021, p. 736978, https://doi.org/10.3389/fmed.2021.736978.

Stoker, Thomas B, and Roger A Barker. “Recent Developments in the Treatment of Parkinson’s Disease.” *F1000Research*, vol. 9, 31 July 2020, p. 862, https://doi.org/10.12688/f1000research.25634.1.

Surmeier, D. James, et al. “Parkinson’s Disease Is Not Simply a Prion Disorder.” *Journal of Neuroscience*, vol. 37, no. 41, 11 Oct. 2017, pp. 9799–9807, https://doi.org/10.1523/JNEUROSCI.1787-16.2017.

Tan, Ai Huey, et al. “The Microbiome–Gut–Brain Axis in Parkinson Disease — from Basic

Research to the Clinic." *Nature Reviews Neurology*, 24 June 2022, https://doi.org/10.1038/s41582-022-00681-2.

Tolosa, Eduardo, et al. "Challenges in the Diagnosis of Parkinson's Disease." *The Lancet Neurology*, vol. 20, no. 5, 1 May 2021, pp. 385–397, https://doi.org/10.1016/S1474-4422(21)00030-2.

Tomlinson, Julianna J, et al. "Holocranohistochemistry Enables the Visualization of α-Synuclein Expression in the Murine Olfactory System and Discovery of Its Systemic Anti-Microbial Effects." *Journal of Neural Transmission*, vol. 124, no. 6, 5 May 2017, pp. 721–738, https://doi.org/10.1007/s00702-017-1726-7.

Tysnes, Ole-Bjørn, and Anette Storstein. "Epidemiology of Parkinson's Disease." *Journal of Neural Transmission*, vol. 124, no. 8, 1 Feb. 2017, pp. 901–905, https://doi.org/10.1007/s00702-017-1686-y.

Vascellari, Sarah, and Aldo Manzin. "Parkinson's Disease: A Prionopathy?" *International Journal of Molecular Sciences*, vol. 22, no. 15, 27 July 2021, p. 8022, https://doi.org/10.3390/ijms22158022.

Villar-Piqué, Anna, et al. "Structure, Function and Toxicity of Alpha-Synuclein: The Bermuda Triangle in Synucleinopathies." *Journal of Neurochemistry*, vol. 139, 11 Sept. 2015, pp. 240–255, https://doi.org/10.1111/jnc.13249.

Visanji, Naomi P, et al. "Gastrointestinal Dysfunction in Parkinson's Disease." *The Lancet Neurology*, vol. 14, no. 6, June 2015, pp. 625–639, https://doi.org/10.1016/s1474-4422(15)00007-1.

Waxman, Elisa A., and Benoit I. Giasson. "Molecular Mechanisms of α-Synuclein Neurodegeneration." *Biochimica et Biophysica Acta (BBA) - Molecular Basis of Disease*,

vol. 1792, no. 7, July 2009, pp. 616–624, https://doi.org/10.1016/j.bbadis.2008.09.013.

Willis, A. W., et al. “Incidence of Parkinson Disease in North America.” *Npj Parkinson’s Disease*, vol. 8, no. 1, 15 Dec. 2022, https://doi.org/10.1038/s41531-022-00410-y.

Xu, Catherine, et al. “The Pathological G51D Mutation in Alpha-Synuclein Oligomers Confers Distinct Structural Attributes and Cellular Toxicity.” *Molecules*, vol. 27, no. 4, 15 Feb. 2022, p. 1293, https://doi.org/10.3390/molecules27041293.

Yi, Meiqi, et al. “Identification and Characterization of an Unexpected Isomerization Motif in CDRH2 That Affects Antibody Activity.” *MAbs*, vol. 15, no. 1, 25 May 2023, https://doi.org/10.1080/19420862.2023.2215364.

Zhang, Cai, et al. “C-Terminal Truncation Modulates α-Synuclein’s Cytotoxicity and Aggregation by Promoting the Interactions with Membrane and Chaperone.” *Communications Biology*, vol. 5, no. 1, 9 Aug. 2022, https://doi.org/10.1038/s42003-022-03768-0.